Eidgenössische Technische Hochschule Zürich
Swiss Federal Institute of Technology Zurich

BACK-TESTING OF TRADING STRATEGIES USING FINANCIAL CRISIS OBSERVATORY OUTPUT

Master Thesis

Tinatin Mamageishvili

February, 2019

Advisors

Dr. Ke Wu
Prof. Dr. Didier Sornette
ETH Zurich: Department of Management, Technology and Economics
Chair of Entrepreneurial Risks

Dr. Fadoua Balabdaoui
ETH Zurich: Department of Mathematics
Seminar for Statistics

Abstract

The goal of this master thesis is to test the predictive power of Log-Periodic Power Law Singularity (LPPLS) indicators designed to detect the emergence and burst of financial bubbles ex-ante. We use the LPPLS warning signals as dynamic risk management tools to time the market. A trading strategy using Financial Crisis Observatory (FCO) output is applied to 27 major equity indices worldwide, covering the time period from December 1994 to July 2018. The investment strategy outperformed the buy-and-hold benchmark in most cases with respect to the Sharpe ratio and significantly reduced drawdowns during the dot-com and the US real estate bubbles. Furthermore, to better understand the mechanics of the indicators when used in practice, we provide a classification of the indices in two classes of short and long price cycles based on the epsilon-drawdown algorithm. We perform hypotheses testing and find evidence that long time-scale LPPLS indicators can better capture the changes in regime when applied to the long-cycled price time-series.

Contents

Chapter 1

Introduction

As an introduction, we will provide an intuitive approach to the formation and burst of bubbles in complex financial systems and argue about the crucial necessity of a good understanding of this phenomena. Financial bubbles are often being debated and misunderstood. Theories on root causes of bubble formations are often varied. In the research paper ”Financial bubbles: mechanisms and diagnostics” [13], financial bubble period is defined as a strong deviation of an asset price from its intrinsic value, which results in an unsustainable growth, accompanied by corrections and rebounds. The crash risk increases as the bubble matures, and finally the system crashes once the bubble formation reaches a critical time.

This phenomena is a consequence of a positive feedback mechanism, herding behaviour, bounded rationality and moral hazard theories. During a bubble course, investors intentionally purchase an asset not for its intrinsic value, but rather by the motive to sell the overvalued asset to another investor at an even higher price. This social phenomena is known as a Greater Fool Theory in finance and economics. The imitation and herding behavior of buyers and sellers is also often compared to Keynesian beauty contest [9], where judges rate a contestant’s appearance based on expectations of other judges’ ratings rather than their own opinions. This concept was introduced to explain price fluctuations in equity markets. Bounded rationality theory states that individual investors have limited time and available information, which makes them take more or less reasonable decisions that are usually not optimal in a given situation. Whereas the moral hazard theory suggests, that in case of a little or no exposition to risks, the behaviour of investors can strongly deviate from what is considered responsible. Such as, if an investor knows that they can take an advantage of a bailout, they may misuse their power to take decisions that are rational only from the individualistic perspective, but may have damaging effects on larger scales. Some argue that this theory explains the formation of the US real estate bubble. Up to now there is no universally accepted theory that could explain the occurrence of bubbles, and each theory represented here can be seen as an incomplete conception of the formation of financial bubbles.

Major financial bubbles have become cultural milestones, as they can trigger bigger problems and spread catastrophic global effects to the economy after the burst. A very good and recent example is the burst of the US housing bubble, which was a result of "Perpetual Money Machine" type of thinking [12] and became the precipitating factor for the financial crisis in 2008, the worst crisis experienced since the great recession in the 1930s. As a consequence stock markets dropped worldwide, many key businesses failed and banking crisis followed. Large financial institutions were damaged globally and their collapse was prevented by bailouts of national government banks. Hence a deep understanding of what happened in the past, predicting what to expect in the future and elaborating on what could be done in order to avoid devastating results is extremely relevant at this age, as we could now be in a phase of another impending financial crisis.

The Financial Crisis Observatory (FCO) is a scientific platform established in August 2008 to pursue a goal of developing science and culture to better understand financial bubbles. The FCO extensively quantifies and analyzes historical time-series of approximately 450 systemic assets and 850 single stocks worldwide. Monthly reports of the analysis across all asset classes is available on their web-page (https://www.ethz.ch/content/specialinterest/mtec/chair-of-entrepreneurial-risks/en/financial-crisis-observatory.html).

Although FCO strongly places itself on the side of Efficient Market Hypothesis [2, 3], they believe that financial markets exhibit certain degrees of inefficiency, especially in the periods when bubbles develop and they systematically test this hypothesis on large scales. The Log Periodic Power Law (LPPL) model, that FCO is equipped with, emerges from statistical physics. It was first introduced to finance by professor Didier Sornette in 1996. The model is used to determine a critical time complex systems reach, i.e. to detect the market crashes ex-ante. Nowadays trading is conducted on different hierarchical levels by many intelligent, interconnected players with different investment styles. Hence, financial markets are complex systems subject to non-linear dynamics, which makes them extremely hard to model [13]. Traditional models assume an exponential growth in price, with a constant growth rate. But in fact, as the positive feedback mechanism and herding behavior fuel further increase in price, the growth rate itself becomes an increasing function in time. As a result an asset price follows a hyperbolic (a.k.a. super-exponential) curve. This kind of growth is not sustainable, meaning that prices can not increase indefinitely. As mentioned above, the LPPL Singularity (LPPLS) model is used to find the time point when the system is most likely to collapse. Note, that models containing the finite time singularity do not gain popularity and are not considered legitimate in economics and finance, as it contradicts the assumption of the existence of the solution at any given time point. But in order to detect the end of the bubble, the non-existence of a solution is the key feature of the LPPLS model.

We review the methodology and define the main model in the second chapter. In the third chapter we discuss the applications of the model and demonstrate the results of a trading strategy back-testing. In the fourth chapter we try to compare two types of indicators and argue about their predictive power within two classes of equity indices. Chapter 5 provides a summary of main conclusions.

Chapter 2

Methodology

Detecting financial bubbles ex-ante is sometimes extremely hard as it is definitely not trivial to tell the difference between a speculative bubble and an innovative transformation. But luckily bubbles usually leave some specific traces behind that enables us to make a timely diagnosis. For this purpose, we introduce the Johansen-Ledoit-Sornette(JLS) [7] model which is the further development of the LPPLS model and is used to describe the price dynamics. It checks whether the price follows super-exponential curve and is designed to find the start and end points of an unsustainable price growth.

2.1 The Log Periodic Power Law Singularity Model

In the bubble phase an asset price largely deviates from its fundamental value and the price dynamics satisfies:

$$\frac{dp_t}{p_t} = \mu_t dt + \sigma_t dW - \kappa dj \tag{2.1}$$

where σ_t is the volatility, dW represents an infinitesimal change in a Brownian motion over the next instant of time, dj is a discontinuous jump ($j = 0$ before and $j = 1$ after the crash) and the parameter κ measures an amplitude of a crash (See [7]). Given that the crash has not yet occurred, we introduce a crash hazard rate $h(t)$, which is the probability that a crash will occur at a given time point t and it is proportional to the expectation of dj: $h(t) := \mathbb{E}[dj]/dt$. We further assume that an asset price satisfies the martingale condition which is equivalent to the rational expectation condition. Multiplying the Eq. (2.1) by p_t and taking the expectation, conditional on the information known up to the time t, yields: $\mathbb{E}_t[dp_t] = \mu_t dt + \sigma_t \mathbb{E}_t[dW_t] - \kappa dj = 0$, which simplifies to:

$$\mu_t = \kappa h(t) \tag{2.2}$$

meaning the return is proportional to the crash hazard rate by the factor of κ and vice versa [14]. Plugging Eq. (2.2) into (2.1) and conditioning on having no crash (i.e. $dj = 0$) yields a differential equation with a solution:

$$\mathbb{E}[\ln\left(\frac{p_t}{p_{t_0}}\right)] = \kappa \int_{t_0}^{t} h(x)dx \tag{2.3}$$

It is apparent from Eq. (2.3) that in order the price to follow the martingale process, the higher the crash probability, the faster price has to increase. Intuition behind it is that investors get higher remuneration for holding a riskier asset. Hence the price growth is driven by the growth of the crash hazard rate $h(t)$ – a crucial parameter that is totally unrestricted. During the bubble run $h(t)$ takes the following form:

$$h(t) = \alpha(t_c - t)^{m-1}\left(1 + \beta\cos\left(\omega\ln(t_c - t) - \varphi^{'}\right)\right), \tag{2.4}$$

with α, β, m, ω, $\varphi^{'}$ and t_c being model parameters. The power law singularity, which is embodied in $\alpha(t_c - t)^{m-1}$, and the log-periodic large scale oscillations are the two structures combined together that lead the process to the critical time t_c. If we combine (2.2) and (2.4) and integrate the expectation of (2.1) conditional on $dj = 0$, we get:

$$\mathbb{E}[\ln p(t)] = A + B(t_c - t)^m + C(t_c - t)^m\cos(\omega\ln(t_c - t) - \varphi), \tag{2.5}$$

where $A = \ln[p(t_c)]$ represents a logarithmic price at a critical time and $B = -\kappa\alpha/m$ (with $B < 0$) represents an amplitude of the power law. In other words, B quantifies the increase in the logarithmic price before the crash and m (with $0 < m < 1$) quantifies the power law with the condition $0 < m < 1$, which ensures the super-exponential growth of price towards t_c. The parameter $C = -\kappa\alpha\beta/\sqrt{m^2 + \omega^2}$ represents the magnitude of oscillations, ω controls the frequency of oscillations and φ is a phase parameter.

For the fitting method, optimization and estimation of the parameters we refer the reader to the following literature [4].

2.2 Calibration of the Model, Derivation of Indicators

In order to estimate the parameter vector $(t_c, \omega, m, \varphi, A, B, C)$, the model is calibrated on the price data using the Ordinary Least Squares (OLS) method (See [1]). Regarding the time scale, we distinguish between long and short time-scale LPPLS indicators. We fix the "present" time, denoted by t_2, up to which the price time-series is given, then we fit the model in the time window (t_1, t_2) with length $dt := t_2 - t_1$ that decreases from 750 trading days to 125 trading days in order to generate the long time-scale indicator. Deriving the short time-scale indicator follows the same process, only the time window (t_1, t_2) shrinks from 125 trading days to 20 trading days. In both cases the starting date t_1 is shifted to the right by the step of 5 trading days, which for each fixed t_2 results in analyzing 126 and 22 time-windows for LPPLS long and short time-scale indicators, respectively. The Table 2.1 summarizes filtering conditions for the parameters. Suggested filters are based on empirical evidence gained from the research on previous bubble investigations [16, 17, 8, 6, 19, 5].

Item	**Notation**	**Search space**	**Filtering condition (Early Warning)**	**Filtering Condition (End Flag)**
Nonlinear Parameters	m	$[0, 2]$	$[0.01, 1.2]$	$[0.01, 0.99]$
	ω	$[1, 50]$	$[2, 25]$	$[2, 25]$
	t_c	$[t_2 - 0.2dt, t_2 + 0.2dt]$	$[t_2 - 0.05dt, t_2 + 0.1dt]$	$[t_2 - 0.05dt, t_2 + 0.1dt]$
Number of oscillations	$\frac{\omega}{2} \ln \left\| \frac{t_c - t_1}{t_2 - t_1} \right\|$	—	$[2.5, +\infty]$	$[2.5, +\infty]$
Damping	$\frac{m\|B\|}{\omega\|C\|}$	—	$[0.8, +\infty]$	$[1, +\infty]$
Relative Error	$\frac{p_t - \widehat{p}_t}{\widehat{p}_t}$	—	$[0, 0.05]$	$[0, 0.2]$

Table 2.1: Search space and filtering conditions to quantify valid LPPLS fits

In order to construct the LPPLS Confidence indicator for the fixed t_2, the fraction of its valid LPPLS fits is calculated. The obtained value is then multiplied by the sign of the median of cumulative returns since the time t_1. Hence the indicator value always lies in the interval $[-1, 1]$. Meaning that if the indicator is positive, we are in a positive bubble run, and if the indicator is negative, we are in a negative bubble phase. Furthermore, regarding the signal produced, we differentiate between two types of indicators: Early Bubble Warning and Bubble End Flag indicators, and as discussed earlier, each one of these has a short and long time-scale versions. It is of our dominant concern to find the signatures of bubbles as early as possible, since a correction or a crash risk increases as the bubble advances to maturity [13]. The Early Bubble Warning indicator is hence a powerful tool to track bubbles from an early stage of their development. A positive (negative) value of the Early Bubble Warning indicator gives a signal of an emerging positive (resp. negative) bubble. The Bubble End Flag indicator is giving a signal if a positive (negative) bubble run is about to end. If the absolute value of this signal is high, it means the price process is not sustainable anymore, and depending on the sign of the indicator, we should expect either a crash or a rebound.

2.2.1 Lagrange Regularization Advancement

A question, how do we know what time point is the inception of a bubble, inspired an improvement of the model that was incorporated in the calibration method of LPPLS indicators in 2017. The LPPLS model only produces valid results if we are in a bubble regime, but if we start calibrating before or after the bubble period, the model may not produce correct signals. Hence, Lagrange regularization approach is combined with the LPPLS model to detect the most optimal starting point t_1^* of a bubble for each fixed pseudo present time t_2. New fits are constructed over the time interval $[t_1^*, t_2]$, with $t_1^* > t_1$. More on the new model estimation and calibration can be read in the research paper by Demos and Sornette [1].

Chapter 3

Backtesting of A Trading Strategy

This thesis is a follow-up work of a master thesis [10], which focused on the long time-scale Early Bubble Warning and Bubble End Flag indicators. In the thesis they developed ”Dragon-Hunting” and ”Bubble Overlay” trading strategies. The first strategy focused on capturing the Dragon Kings [11], very rare and also tremendously powerful in impact and size financial bubbles, that unlike the Black Swans [18] are to some degree predictable. The second strategy mainly aimed to avoid negative bubbles rather than being opportunistic. The Dragon Hunting and Bubble Overlay strategies outperformed the Buy and Hold strategy in terms of the Sharpe Ratio in respectively 23 and 22 cases out of 27. The author made an argument that the out-performance was mostly due to two large bubbles that took place in the last two decades. Now we are going to incorporate the short time-scale indicators into the game and try to test their predictive power alongside with the long time-scale indicators. We also aim to make a comparison between the long and short time-scale indicators and argue about their performances in different index classes.

3.1 Data

For this analysis we use a daily closing price time-series of 27 major equity indices given in Table 3.1. Data is downloaded from Reuters Datastream and Reuters EIKON and it stretches roughly 23 years, from December 1994 to July 2018. The indicators are calculated on the data, using the new Lagrange regularization approach. Additionally, we use the return time series of the US 3-month Treasury Bonds for the same time period, available at:

https://fred.stlouisfed.org/series/DTB3.

Equity Indices		
Region	Codename	Country
Europe	AEX	Netherlands
	ATX	Austria
	BEL_{20}	Belgium
	BUX	Hungary
	CAC_{40}	France
	DAX_{30}	Germany
	EURO $STOXX_{50}$	Europe
	$FTSE_{100}$	United Kingdom
	IBEX	Spain
	$OMXS_{30}$	Sweden
	PSI_{20}	Portugal
	SMI	Switzerland
US	DOW JONES INDUSTRIALS	US
	NASDAQ	US
	NYSE	US
	$RUSSELL_{2000}$	US
	S&P 500	US
Asia	BANGKOK S.E.T.	Thailand
	Hang Seng	Hong Kong
	KOSPI	South Korea
	$NIKKEI_{225}$	Japan
	SHANGHAI SE A SHARE	China
	TAIEX	Taiwan
South America	BOVESPA	Brazil
	MERVAL	Argentina
International	MSCI AC WORLD	-
	MSCI WORLD	-

Table 3.1: Major 27 Equity Indices used for backtesting the strategy

3.2 Trading Strategy

For this investment strategy, we use the Early Bubble Warning and the Bubble End Flag indicators on both time-scales. We want to remind the reader an intuition behind the indicators: once the Early Bubble Warning gets positive (negative), it means that the positive (resp. negative) bubble patterns are starting to emerge, and the signal gets stronger as the bubble matures. The Bubble End Flag signal larger than 5% is a strong indication that there is a risk the positive bubble run will end and either a crash or a substantial correction will occur [14]. The higher the signal, the higher the crash risk. The Bubble End Flag signal being less than -5% translates into a high likelihood of a rebound.

We start from smoothing all four indicators with a 100-day simple moving average (MA_{100}). Since the indicators are very volatile, this step ensures to avoid redundant trades but it also keeps the main signal produced by the indicators. Having a signal at time t, we trade at time $t+1$ close price. In order to target potential gains, we consider two conditions to enter the market.
Condition I: We invest in an equity index at time $t+1$ if at least one of the following two cases is true at time t:

- Early Bubble Warning *long* time-scale signal is larger than α
- Early Bubble Warning *short* time-scale signal is larger than α

with $\alpha \in (-0.01, 0, 0.01)$. The value of α, that gives the best performance of the strategy in terms of the Sharpe Ratio, is chosen individually for each index. In order to have more potential gains, we continue to pursue an opportunistic goal and hunt for positive bubbles. For this purpose, we furthermore observe the Bubble End Flag on long and short time-scales. We look for the negative Bubble End Flag signals.
Condition II: We enter the market at time $t+1$ and stay in the market for 100 consecutive trading days if both of the following are simultaneously true at time t:

- Bubble End Flag *long* time-scale signal is less than -0.05
- Bubble End Flag *short* time-scale signal is negative.

which would be a sufficient signal for a rebound, as the negative Bubble End Flag produces a warning for the end of a negative bubble. The short time-scale Bubble End Flag indicator produces non-zero signal less frequently than its long time-scale analogue. Also, smoothing out the indicators almost diminishes the short time-scale Bubble End Flag indicator signal, this is the reason why we set a milder threshold for this indicator.

To sum up, if the Condition I holds true at time t but the Condition II does not, then we enter the market at time $t+1$ for one day. If the Condition II is fulfilled, we enter the market and stay in for 100 consecutive days, independently from the Condition I. If none of the two conditions hold true, then we are out of the market at time $t+1$. If we are not investing in an equity index, we invest in the risk-free 3-Month US Treasury Bills. Transaction costs (0.1%) are included in the calculation of the strategy performance.

We measure a performance of the strategy with the Sharpe ratio and the Calmar ratio. The Sharpe ratio is a common measure of a portfolio performance and is defined as:

$$\textit{Sharpe Ratio} = \frac{r_a - r_f}{\sigma_a} \tag{3.1}$$

with r_a being a risk associated with the asset we invest in, r_f being a risk-free rate and σ_a being a volatility of the asset price. Sharpe Ratio measures risk-adjusted returns of an investment. In the numerator we have the excess to the "zero-risk" rate we are willing to take, which is then corrected by the total volatility σ_a. The higher the Sharpe ratio, the more attractive risk-adjusted returns of the investment will be. Another metric to measure the performance of an investment strategy on a risk-adjusted basis is a Drawdown ratio (also called Calmar ratio). It is defined as:

$$\textit{Drawdown Ratio} = \frac{\textit{Annual Return - Annual Risk-Free Rate}}{\textit{AverageLargestDrawdown}} \tag{3.2}$$

Just like the Sharpe ratio, this is an important tool to compare two strategies. A high Calmar ratio indicates low risk, whereas a low Calmar ratio suggests a high risk of drawdowns.

3.2.1 Results of the trading Strategy

We apply our strategy to 27 equity indices. Performance results are shown in full in the appendix. Here we only present the results for seven major equity indices located in Europe, Asia and the USA (see Figures 3.1 – 3.7). The strategy outperforms 22 indices out of 27 with respect to the Sharpe ratio and it outperforms 23 indices out of 27 with respect to the Drawdown ratio. We fix the Early Bubble Warning entry thresholds α for each index and check the robustness of the strategy with respect of the second entry strategy, we vary the parameters and represent the results in the Table 3.2.

Nr. of	**Exit Threshold for Bubble End Flag Long**								
Days	**0**	**-0.01**	**-0.02**	**-0.03**	**-0.04**	**-0.05**	**-0.06**	**-0.08**	**-0.1**
20	19	22	20	21	21	21	21	21	21
50	19	22	20	21	21	22	21	21	21
75	20	22	20	21	21	22	22	21	21
100	20	23	20	21	21	22	22	21	21
120	19	22	20	20	21	22	21	21	21
150	20	21	19	20	20	21	21	21	21
200	20	22	20	20	20	21	21	21	21

Table 3.2: The table illustrates sensitivity in the out-performance of the strategy with respect to changes in the threshold for the Bubble End Flag long time-scale indicator (horizontal axis) and the number of days we stay invested in the market (vertical axis). The intersection of our parameter choices is highlighted.

The Table shows that entering the market if the End Flag long time-scale signal is less than -0.01, and keeping other parameters fixed, results in out-performing 23 indices out of 27. Although we made an argument that the Bubble End Flag signal smaller than -0.05 was a good indication of a rebound, it holds true already below the value -0.01. This is explained by the fact that we smoothed the indicator by the window size of 100 trading days. Hence already a small signal is enough for us to take an action. It is noteworthy that the Condition II rarely holds true. If we remove it from the strategy and leave the first condition for entering long, the strategy outperforms 21 indices out of 27. Adding the second condition increases the out-performance by one index and it also increases the Sharpe ratios for most indices. It certainly helps the strategy perform better, but the improvement is not too significant. Hence we can argue that the Early Bubble Warning indicator is the main contributor to the out-performance for this strategy.

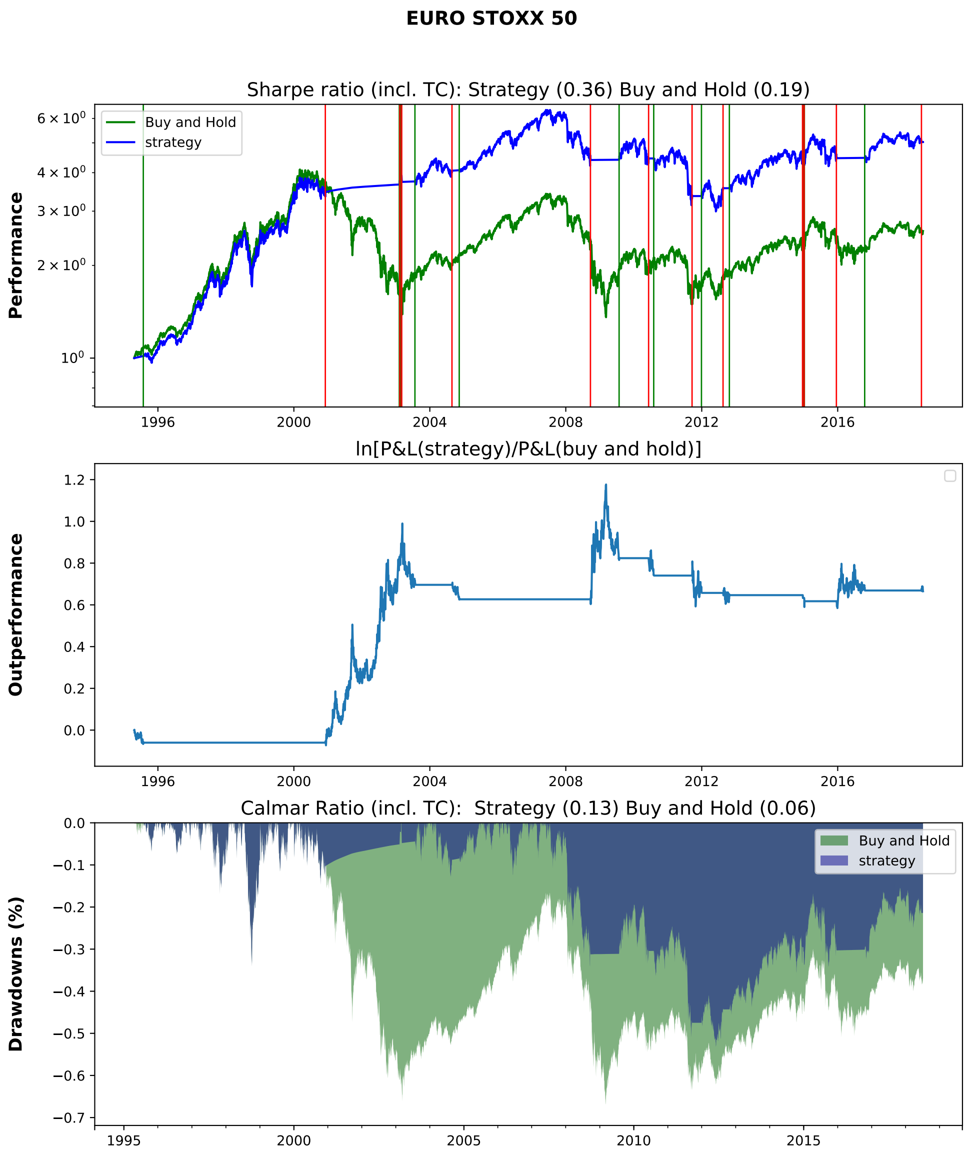

Figure 3.1: Performance of the trading strategy for the equity index **EURO STOXX 50** during the time-period *December 1994 - July 2018*. The first panel of the figure represents Profit and Loss (P&L) plots of the buy-and-hold benchmark (in green) and our strategy (in blue), quantified with the Sharpe ratios. The second panel represents the performance of the strategy relative to the benchmark. The third panel represents the drawdowns of both the strategy and the benchmark, quantified with the Calmar ratios. Early Bubble Warning entry threshold $\alpha = 0$.

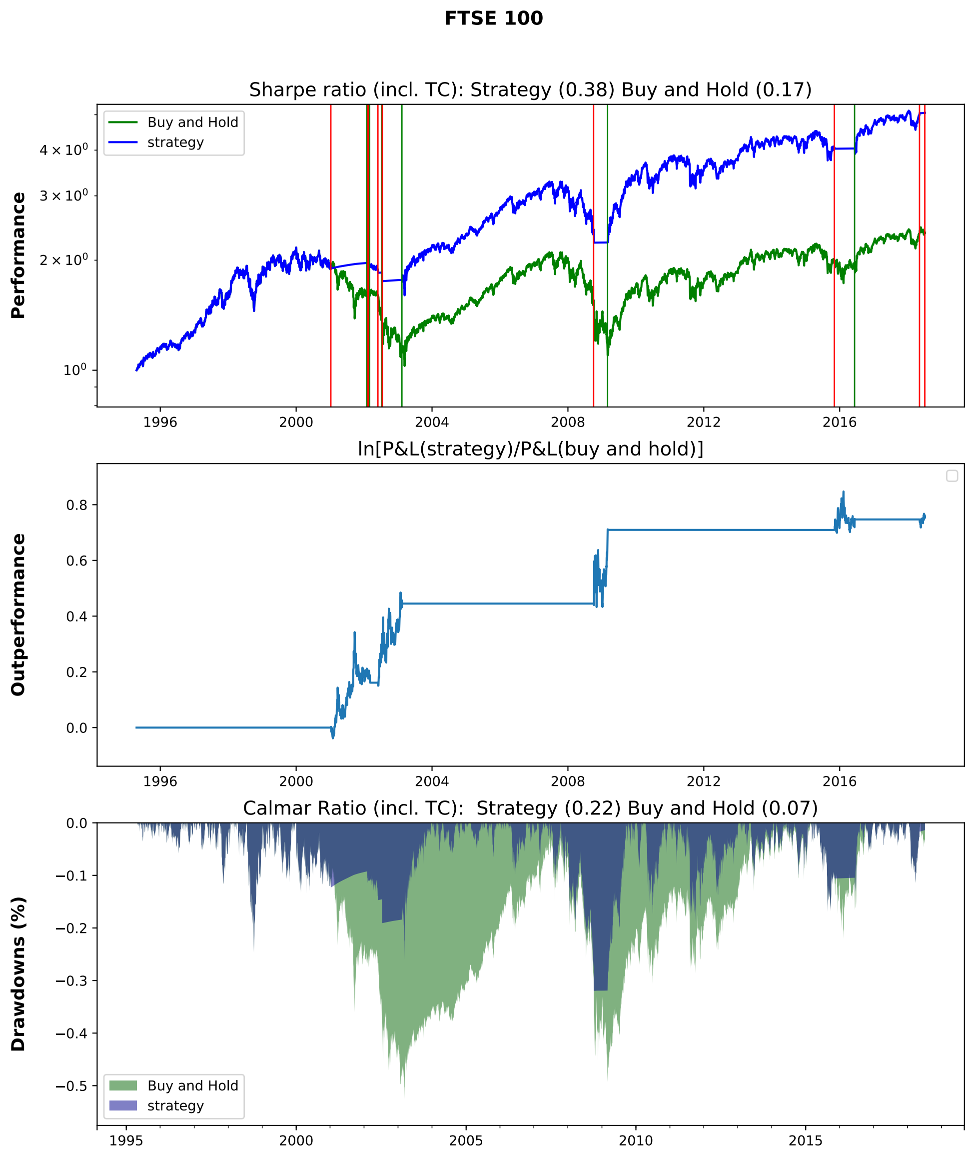

Figure 3.2: Performance of the trading strategy for the equity index **FTSE 100** during the time-period *December 1994 - July 2018*. The first panel of the figure represents Profit and Loss (P&L) plots of the buy-and-hold benchmark (in green) and our strategy (in blue), quantified with the Sharpe ratios. The second panel represents the performance of the strategy relative to the benchmark. The third panel represents the drawdowns of both the strategy and the benchmark, quantified with the Calmar ratios. Early Bubble Warning entry threshold $\alpha = -0.01$.

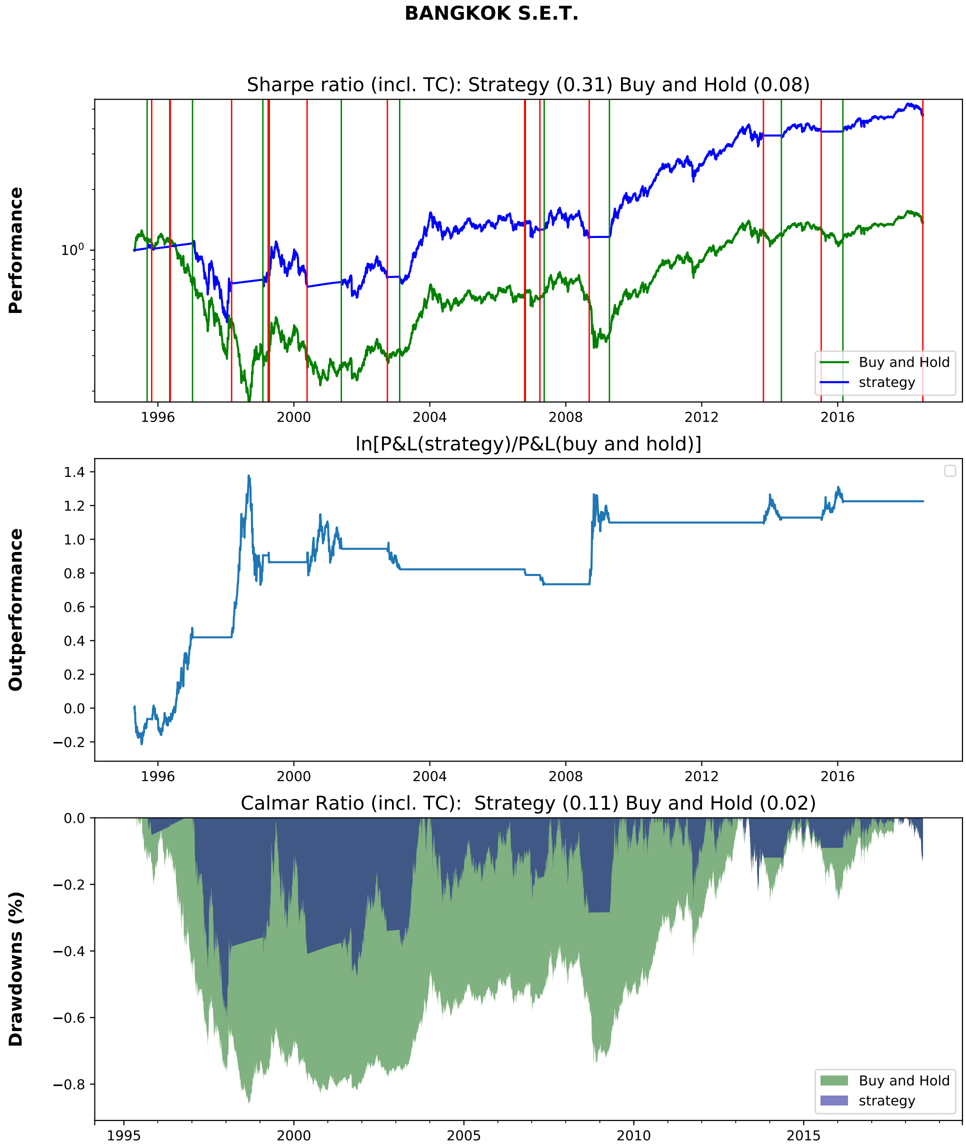

Figure 3.3: Performance of the trading strategy for the equity index **Bangkok** during the time-period *December 1994 - July 2018*. The first panel of the figure represents Profit and Loss (P&L) plots of the buy-and-hold benchmark (in green) and our strategy (in blue), quantified with the Sharpe ratios. The second panel represents the performance of the strategy relative to the benchmark. The third panel represents the drawdowns of both the strategy and the benchmark, quantified with the Calmar ratios. Early Bubble Warning entry threshold $\alpha = 0$.

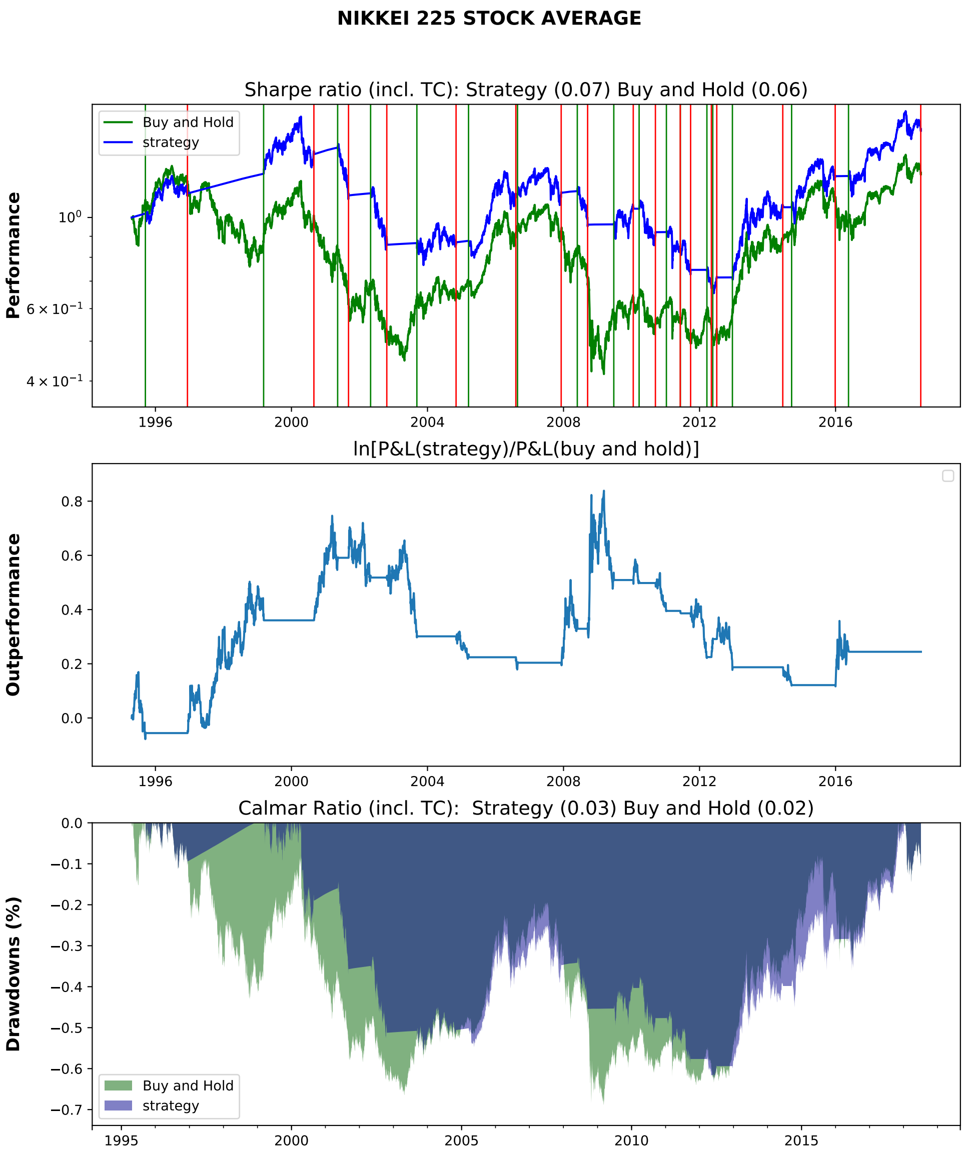

Figure 3.4: Performance of the trading strategy for the equity index **Nikkei** during the time-period *December 1994 - July 2018*. The first panel of the figure represents Profit and Loss (P&L) plots of the buy-and-hold benchmark (in green) and our strategy (in blue), quantified with the Sharpe ratios. The second panel represents the performance of the strategy relative to the benchmark. The third panel represents the drawdowns of both the strategy and the benchmark, quantified with the Calmar ratios. Early Bubble Warning entry threshold $\alpha = 0.01$.

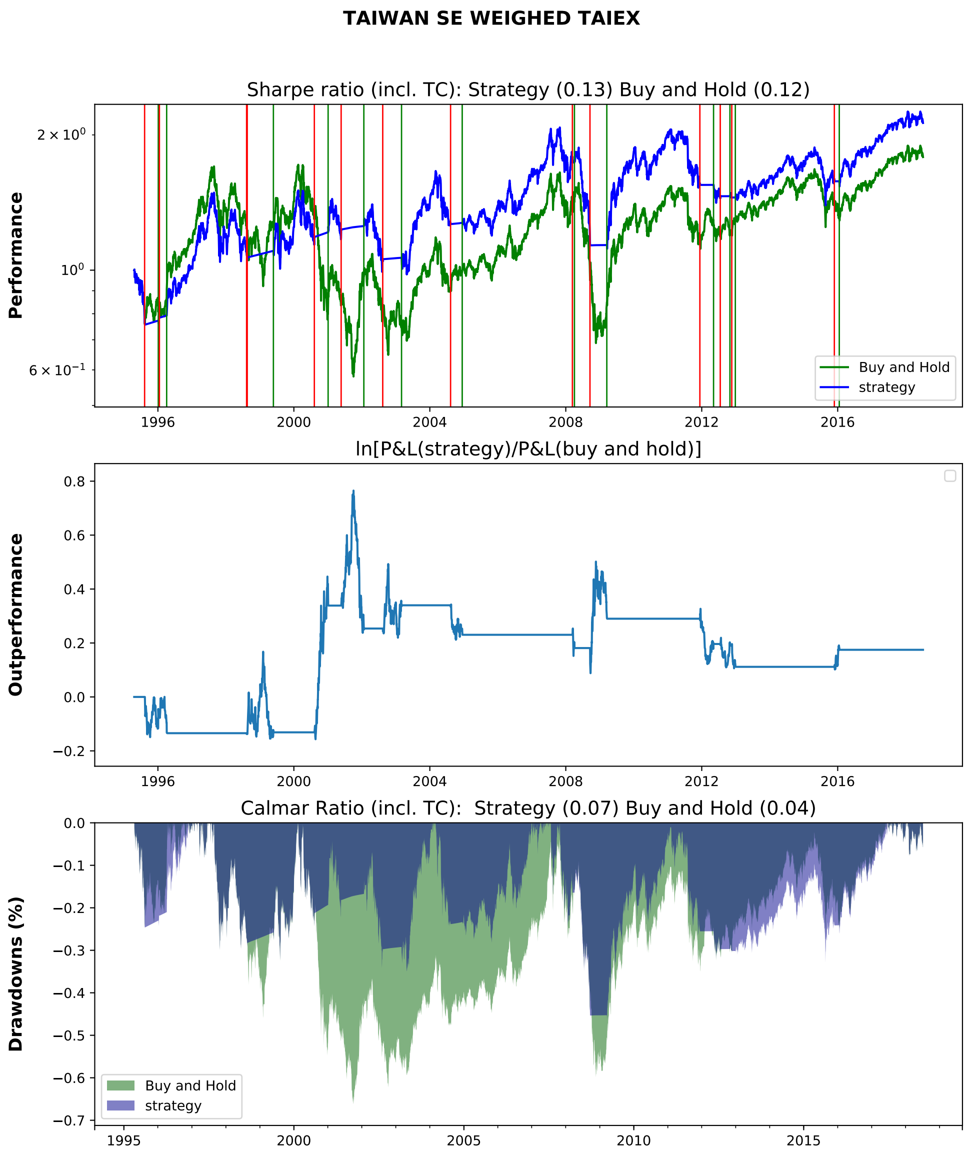

Figure 3.5: Performance of the trading strategy for the equity index **Taiwan** during the time-period *December 1994 - July 2018*. The first panel of the figure represents Profit and Loss (P&L) plots of the buy-and-hold benchmark (in green) and our strategy (in blue), quantified with the Sharpe ratios. The second panel represents the performance of the strategy relative to the benchmark. The third panel represents the drawdowns of both the strategy and the benchmark, quantified with the Calmar ratios. Early Bubble Warning entry threshold $\alpha = -0.01$.

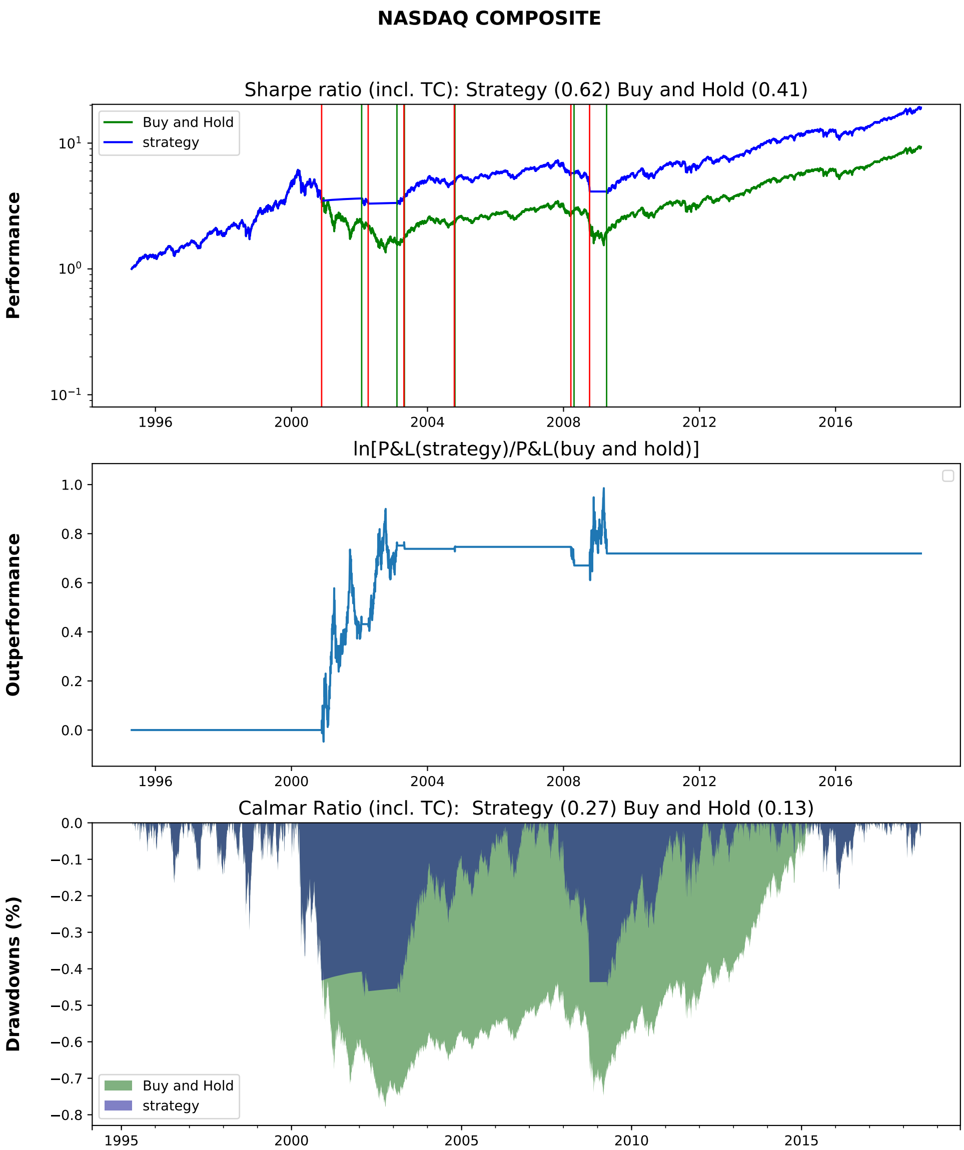

Figure 3.6: Performance of the trading strategy for the equity index **Nasdaq** during the time-period *December 1994 - July 2018*. The first panel of the figure represents Profit and Loss (P&L) plots of the buy-and-hold benchmark (in green) and our strategy (in blue), quantified with the Sharpe ratios. The second panel represents the performance of the strategy relative to the benchmark. The third panel represents the drawdowns of both the strategy and the benchmark, quantified with the Calmar ratios. Early Bubble Warning entry threshold $\alpha = -0.01$.

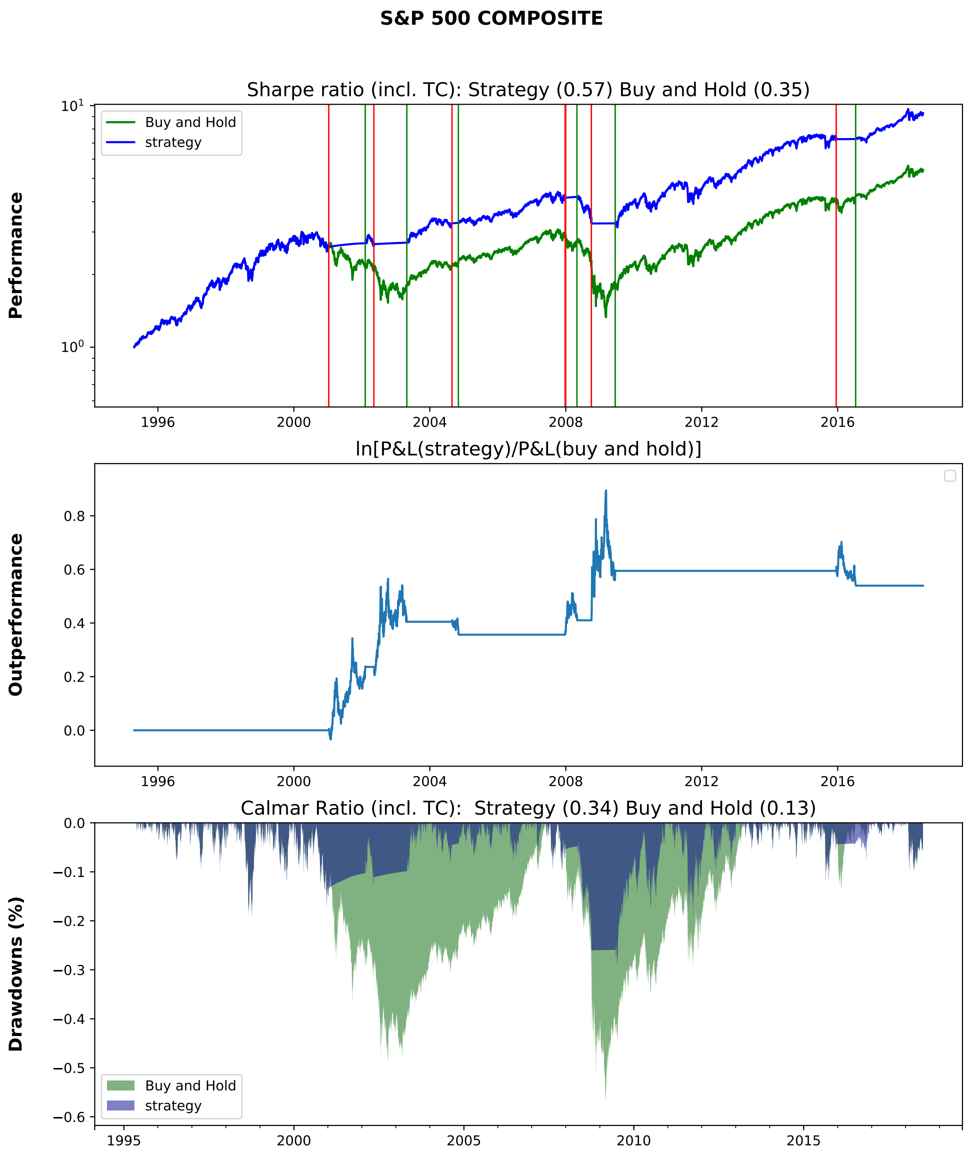

Figure 3.7: Performance of the trading strategy for the equity index **S&P 500** during the time-period *December 1994 - July 2018*. The first panel of the figure represents Profit and Loss (P&L) plots of the buy-and-hold benchmark (in green) and our strategy (in blue), quantified with the Sharpe ratios. The second panel represents the performance of the strategy relative to the benchmark. The third panel represents the drawdowns of both the strategy and the benchmark, quantified with the Calmar ratios. Early Bubble Warning entry threshold $\alpha = 0.01$.

Index name	Sharpe ratio		Calmar ratio		Max-DD	
	Strategy	BM	Strategy	BM	Strategy	BM
AEX	0.4	0.22	0.14	0.07	-51.3%	-71.6%
MERVAL	0.92	0.63	0.6	0.25	-42.7%	-76.8%
ATX	0.22	0.24	0.08	0.07	-59.7%	-71.7%
BANGKOK S.E.T.	0.31	0.08	0.11	0.02	-60.5%	-85.9%
BEL 20	0.14	0.2	0.06	0.06	-57.1%	-67.9%
BOVESPA	0.56	0.5	0.23	0.21	-65.0%	-65.0%
BUX	0.67	0.58	0.27	0.22	-58.1%	-68.6%
DAX 30	0.5	0.35	0.26	0.11	-37.6%	-72.7%
DOW JONES	0.5	0.38	0.28	0.14	-30.4%	-53.8%
EURO STOXX 50	0.36	0.19	0.13	0.06	-53.2%	-66.9%
CAC 40	0.32	0.2	0.12	0.07	-52.7%	-65.3%
FTSE 100	0.38	0.17	0.22	0.07	-32.0%	-52.6%
HANG SENG	0.22	0.23	0.07	0.08	-64.8%	-65.2%
IBEX 35	0.16	0.23	0.05	0.08	-64.6%	-62.6%
KOSPI	0.25	0.19	0.13	0.05	-41.3%	-72.5%
MSCI AC WORLD	0.44	0.24	0.2	0.08	-34.4%	-59.6%
MSCI WORLD	0.48	0.25	0.21	0.08	-34.9%	-59.1%
NASDAQ	0.62	0.41	0.27	0.13	-47.7%	-77.9%
NIKKEI 225	0.07	0.06	0.03	0.02	-62.8%	-68.9%
NYSE	0.4	0.31	0.18	0.11	-40.0%	-59.0%
OMXS30	0.5	0.32	0.25	0.1	-39.4%	-72.6%
PSI-20	0.56	0.04	0.26	0.02	-35.0%	-71.3%
RUSSELL 2000	0.31	0.36	0.13	0.13	-48.6%	-59.9%
S&P 500	0.57	0.35	0.34	0.13	-28.7%	-56.8%
SHANGHAI	0.3	0.28	0.13	0.09	-52.9%	-72.0%
SMI	0.4	0.25	0.18	0.09	-39.1%	-56.3%
TAIEX	0.13	0.12	0.07	0.04	-46.3%	-66.2%

Table 3.3: The table compares performances of the strategy and the benchmark (BM) for each index with respect to the Sharpe ratio, the Calmar ratio and the maximal draw-down(Max-DD). Green entries show that the strategy outperformed the benchmark. Red entries highlight the cases where the benchmark outperformed our strategy.

Chapter 4

Testing of hypothesis based on epsilon-drawdown classification

In this chapter we aim to make one step forward to understand the mechanics behind the long and short time-scale LPPLS indicators. After executing a few back-testing strategies, it became apparent that with some equity indices the short time-scale indicators were performing better than the long time-scale indicators and the other way around. We want to check, whether long (short) time scale indicators perform significantly better with the indices that have long-cycle (resp. short-cycle) price movements. In order to classify the index price time-series as either long or short cycled, we use the epsilon-drawdown method. See [15].

4.1 Epsilon Drawdowns

Drawdowns are useful metrics to quantify the risk associated with the systematic extreme events. Drawdowns (drawups) are defined as a persistent decrease (resp. increase) in the price over consecutive time intervals. Drawdowns (drawups) are calculated as the sum of consecutive negative (resp. positive) returns. Drawdowns and drawups alternate, one is followed by the other and vice versa. Traditional drawdowns are very rigid and sensitive to noise, in the sense that every tiny upward movement of the price will break a large drawdown into parts. Hence a more robust measure of drawdowns, the so-called ε-drawdown was introduced by Johansen and Sornette (2010). An ε-drawdown is defined as a traditional drawdown, except positive returns smaller than some pre-defined threshold controlled by the parameter $\varepsilon > 0$ are considered as "noise" and do not end a drawdown run. For $\varepsilon = 0$ we have a traditional notion of a drawdown.
Technically, the procedure is as follows: Consider a total time interval $[t_1, t_2]$. We divide it into $N = \lfloor (t_2 - t_1)/\Delta t \rfloor$ time periods of length Δt. We can con-

struct returns from log-price time-series on discrete time intervals Δt as

k=k$_0 = 1$ is defined as the beginning of a drawup if $r_1 > 0$ and a drawdown if $r_1 < 0$. Then for each $k > k_0$ we calculate the cumulative sum:

$$p_{k_0,k} = \sum_{i=k_0}^{k} r_i \tag{4.2}$$

and we test the largest deviation $\delta_{k_0,k}$ of the price trajectory from the previous extremum:

$$\delta_{k_0,k} = \begin{cases} p_{k_0,k} - \min\limits_{k_0 \le i \le k} p_{k_0,i} & \text{for drawdowns} \\ \max\limits_{k_0 \le i \le k} p_{k_0,i} - p_{k_0,k} & \text{for drawups} \end{cases} \tag{4.3}$$

The process stops as soon as $\delta_{k_0,k}$ becomes larger than ε:

$$\delta_{k_0,k} > \varepsilon = \varepsilon_0 \sigma \tag{4.4}$$

More specifically, if we are in a drawdown phase and $p_{k_0,k} - \min_{k_0 \le i \le k} p_{k_0,i} > \varepsilon$, we end the drawdown and enter the drawup phase. In equation (4.4) ε_0 is a constant and σ is the measure of recent volatility, defined as:

$$\sigma = \sqrt{\frac{1}{N} \sum_{k=0}^{N} r_k^2} \tag{4.5}$$

.

Descriptive statistics of drawdowns

The drawdowns and drawups are characterized by:

- duration: $\tau = (k_{end} - k_{start})\Delta t$;
- size: $\Delta P = |P(t_1 + k_{end}\Delta t) - P(t_1 + k_{start}\Delta t)|$;
- return: $r = |\log P(t_1 + k_{end}\Delta t) - \log P(t_1 + k_{start}\Delta t)|$;
- normalized return: $r_{norm} = r/\sigma$, with σ being the volatility of the previous trading day, defined as in Eq. (4.5);
- speed: $v = r/\tau$.

4.1.1 Classification of Equity Indices

In order to see a large picture in the price movements of each equity index, we made the parameter choice $\Delta t = 300$ trading days and $\varepsilon_0 = 10$. The first parameter ensures that the algorithm takes into account the variation of the prices on a long time interval and the second parameter is large enough to ignore small price changes in the opposite direction, which allows us to see larger trends of upward or downward motion in the price time-series.
We take into account the durations of the drawdowns (drawups) modelled by the parameter τ, which in our case is measured in the number of days. For each instrument, we observe the distribution of the duration τ. The figure 4.1 illustrates the result of this procedure for one of the equity indices.

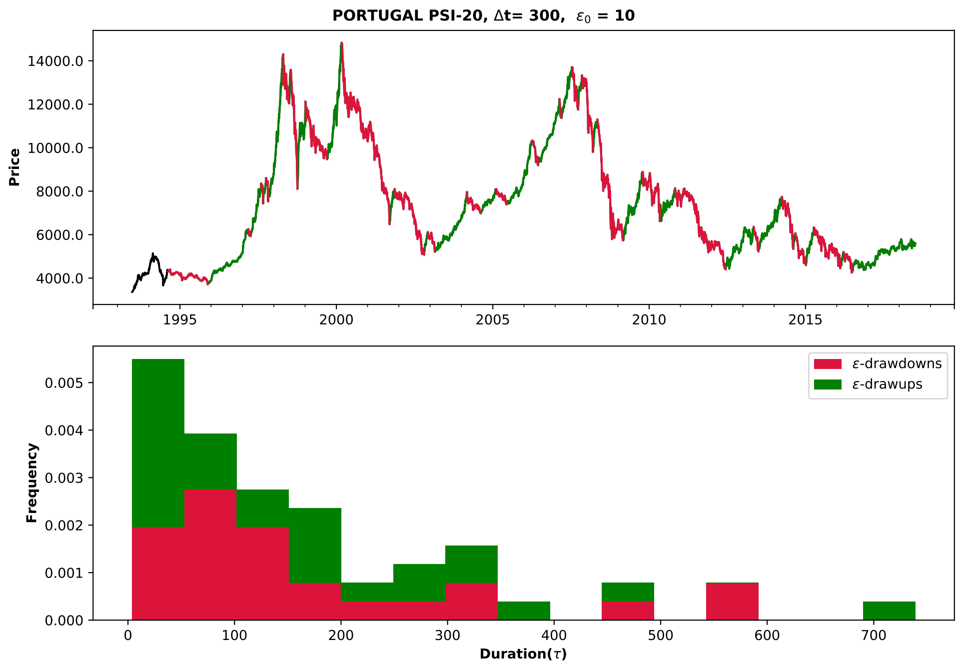

Figure 4.1: The first plot is the visualization of Epsilon-Drawdown Algorithm for Portugal PSI price time-series. The second plot is a (normalized) histogram of drawdown and drawup durations. This index price time series was classified as short-cycled.

In order to classify an index price time-series as short or long cycled, we apply a restriction to the right tail of the distribution. We classify an index short-cycled if the $q_{0.9} < 450$ and $q_{0.95} < 800$, otherwise it belongs to the long cycle class. Here $q_{0.9}$ and $q_{0.95}$ are the 0.9 and 0.95 quantiles of the distribution of durations (τ). This way, 14 equity indices out of 27 indices are classified as short cycled and 13 indices – as long cycled. Note, that if we make the ε threshold smaller, we need to also adjust the values of the quantile thresholds to this parameter for our classification to stay unchanged.

Also, there are other possibilities to classify indices into long and short cycles using other descriptive statistics defined above, such as the *speed* or the *size* of the draw-downs(-ups).

4.2 Hypothesis testing

4.2.1 Bubble Overlay strategy for short cycled indices

We consider "Bubble Overlay" trading strategy discussed in the previous Master's thesis [10]. The strategy uses the smoothed (MA_{100}) Early Bubble Warning indicator on a long time-scale as an input. The author is investing in an equity index if the MA_{100} is non-negative. They reduce the exposure by one fourth if the indicator is less than 0. If it gets less than -0.01 or -0.02, the exposure is reduced by one half and by three quarters, respectively. If the indicator falls below the threshold -0.03, the author exits the market completely and invests in the 3-month US treasury bills instead.

In the Table 3.1 you can see 14 short cycled indices and their Sharpe ratios generated by the Bubble Overlay strategy. In the column "LPPLS Short" ("LPPLS Long") you can see the Sharpe ratios of the indices generated by the strategy with the short (resp. long) time-scale indicator as an input. In the last column one can see the Sharpe ratios of the Buy and Hold strategy, as a benchmark.

	LPPLS Short	LPPLS Long	Benchmark
ATX	0.32	0.48	0.27
BANGKOK S.E.T.	0.48	0.43	0.34
BEL 20	0.03	0.07	0.06
KOSPI	0.31	0.27	0.3
MERVAL	0.89	0.92	0.73
MSCI AC WORLD	0.37	0.42	0.16
MSCI WORLD	0.33	0.43	0.16
NASDAQ	0.53	0.45	0.3
NIKKEI 225	0.05	0.05	0.11
NYSE	0.25	0.24	0.18
PSI-20	0.17	0.02	-0.16
RUSSELL 2000	0.26	0.28	0.34
SHANGHAI	0.25	0.18	0.22
TAIEX	0.19	0.06	0.11

Table 4.1: The table illustrates the Sharpe ratios of the 14 equity indices in a **Short Cycle**, generated by "Bubble Overlay" strategy using LPPLS short and LPPLS long time-scale Early Bubble Warning indicators.

We compare the performances of LPPLS Short and LPPLS Long within this class. The sample average of the Sharpe ratios using LPPLS Short indicator ($\overline{X}_{LPPLS-Short} = 0.316$) is greater than the sample average using LPPLS Long indicator ($\overline{X}_{LPPLS-Long} = 0.307$). We want to test whether this difference has any statistical significance.

We state the following hypotheses testing problem:

$$H_0 : \mu_1 = \mu_2 \qquad H_1 : \mu_1 > \mu_2 \tag{4.6}$$

With μ_1 being the mean of the Sharpe ratios of LPPLS Short strategy, and μ_2 – the mean of Sharpe ratios of LPPLS Long strategy. We set the test level (type-I-error) to the standard $\alpha = 0.05$. The paired samples t-test gives the following output:

T-statistic: 0.407091 P-value: 0.345281

Since the reported p-value is larger than the test level α, we can not reject the Null Hypothesis. Although for some short cycled indices, the LPPLS short time-scale indicator indeed performs better than the LPPLS long-time scale indicator.

Now instead of the parametric paired t-test, which needs normality assumption, we use a non-parametric Mann-Whitney-U test, which tests if it is equally likely that a randomly selected value from one sample will be less than or greater than a randomly selected value from a second sample. We state the same testing problem (4.6) and we get the following result:

Statistic=100.0 P-value=0.472511

Neither of the two tests allow us to reject the Null Hypothesis at the test level $\alpha = 0.05$. So we deduce that the Bubble Overlay strategy produces the same results with the LPPLS long and LPPLS short-time scale indicators within the short-cycled class of indices.

4.2.2 Bubble Overlay Strategy for Long Cycled indices

We can In the Table 4.2 we can observe 13 long-cycled indices, and their corresponding Sharpe ratios produced by Bubble Overlay Strategy using LPPLS Short and LPPLS Long time-scale Early Bubble Warning indicators.

The Sharpe ratio sample average of the LPPLS Short ($\overline{X}_{LPPLS-Short} = 0.237$) is smaller than the sample average of the LPPLS Long ($\overline{X}_{LPPLS-Long} = 0.31$). Hence we modify our hypotheses accordingly and state the following testing problem for the same test level $\alpha = 0.05$, with the right sided alternative:

$$H_0 : \mu_1 = \mu_2 \qquad H_1 : \mu_1 < \mu_2 \tag{4.7}$$

	LPPLS Short	LPPLS Long	Benchmark
AEX	0.09	0.19	0.03
BOVESPA	0.41	0.54	0.44
BUX	0.49	0.54	0.42
DAX 30	0.33	0.35	0.24
DOW JONES INDUSTRIALS	0.29	0.4	0.24
EURO STOXX 50	0.15	0.2	0.03
CAC 40	0.24	0.21	0.09
FTSE 100	0.12	0.11	0.06
HANG SENG	0.32	0.25	0.23
IBEX 35	-0.09	0.05	0.04
OMXS 30	0.33	0.48	0.19
SP 500	0.26	0.52	0.21
SWISS MARKET	0.14	0.19	0.06

Table 4.2: The table illustrates 13 equity indices in a **Long Cycle** and their Sharpe ratios, generated by "Bubble Overlay" strategy using LPPLS short and LPPLS long time-scale Early Bubble Warning indicators.

Again, with μ_1 and μ_2 being the population means of the Sharpe ratios of respectively LPPLS Short and LPPLS Long strategies.

The paired samples t-test gives the following output:

T-statistic: 2.99172 P-value: 0.00561

Since the reported P-value is smaller than α, we reject the Null Hypothesis.

We test the same hypotheses at the same test level (0.05) with the non-parametric U-test. Which results in:

Statistic=47.5 P-value=0.030573

The non-parametric test also agrees with the paired t-test decision rule. Hence we reject the H_0 with confidence and state that in the long-cycled class of indices, using the LPPLS Long time-scale Early Bubble Warning indicator may give better results in terms of Sharpe ratios, hence will have higher predictive power. Although we believe that both alternative hypotheses hold true, we also want to state, that the experiment is too small to prove or disprove either of the two hypotheses. Right now we only produced one trading strategy with two different inputs and made a comparison between the outputs within short and long-cycled classes, but the topic is vast and needs more experiments to be run. The more data we have from both classes to analyze, the more reliable the answers will be. For now, we consider these lines as an opening of the topic for further research.

Chapter 5

Conclusion

Back-testing of the trading strategy involving all indicators showed a significant decrease in drawdowns mainly on the expense of two major bubbles that took place in the last two decades. The dot-com and the US housing bubbles were most of the time successfully captured by the LPPLS indicators. As a result, 22 out of 27 equity indices outperformed the benchmark with respect to the Sharpe Ratio. Results of the preceding Master thesis indicate that the long time-scale indicators did not perform well enough on the equity indices located in Asia. Reproducing one of the trading strategies with the short time-scale LPPLS indicator improved the performances of the mentioned indices. All Asian indices except for Nikkei outperformed the benchmark with respect to the Sharpe ratio (See Table 4.2.1). This could be due to the fact that Asian indices are classified as short-cycled, hence short time-scale indicators could better capture the bubble patterns on such instruments. Although we failed to reject one of the null hypothesis (4.6), we believe that in case of conducting enough experiments, we will be able to see significant results.

As we have seen, bubbles emerge on different time-scales. According to the back-testing results of both theses, the LPPLS indicators are successful at hunting massive bubbles, so called Dragon Kings, but those do not happen often enough for investors to rely only on the LPPLS signals. Hence, we believe that in order to reduce or even in some cases completely avoid huge losses, these novel indicators will be a valuable addition to the trading indicators that have become traditional due to their success in applications.

Appendix A

Investment Strategy Performances

Here we present performances of the investment strategy described in Chapter 3.2. For each index we present a plot with three panels. In the first panel one can see the Profit & Loss for buy-and-hold (in green) and our investment strategy (in blue). Green vertical lines represent the time when we entered the market. Red vertical lines represent the exit times. The second panel represents the performance of the strategy relative to the benchmark. The last panel demonstrates the drawdowns of both strategies quantified with the Calmar ratio (see figures A.1 – A.20).

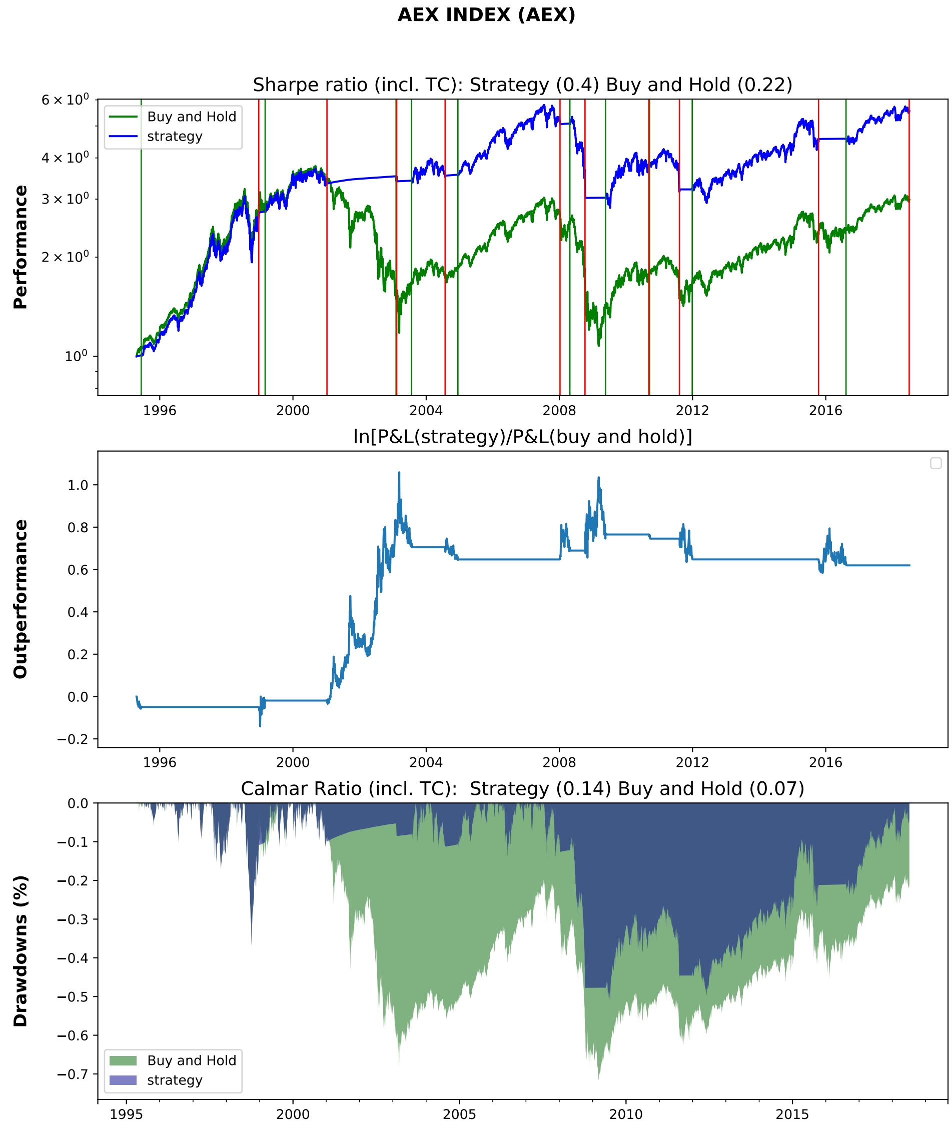

Figure A.1: Performance of the trading strategy for the equity index **AEX** during the time-period *December 1994 - July 2018*. Early Bubble Warning entry threshold $\alpha = 0.01$.

ARGENTINA MERVAL

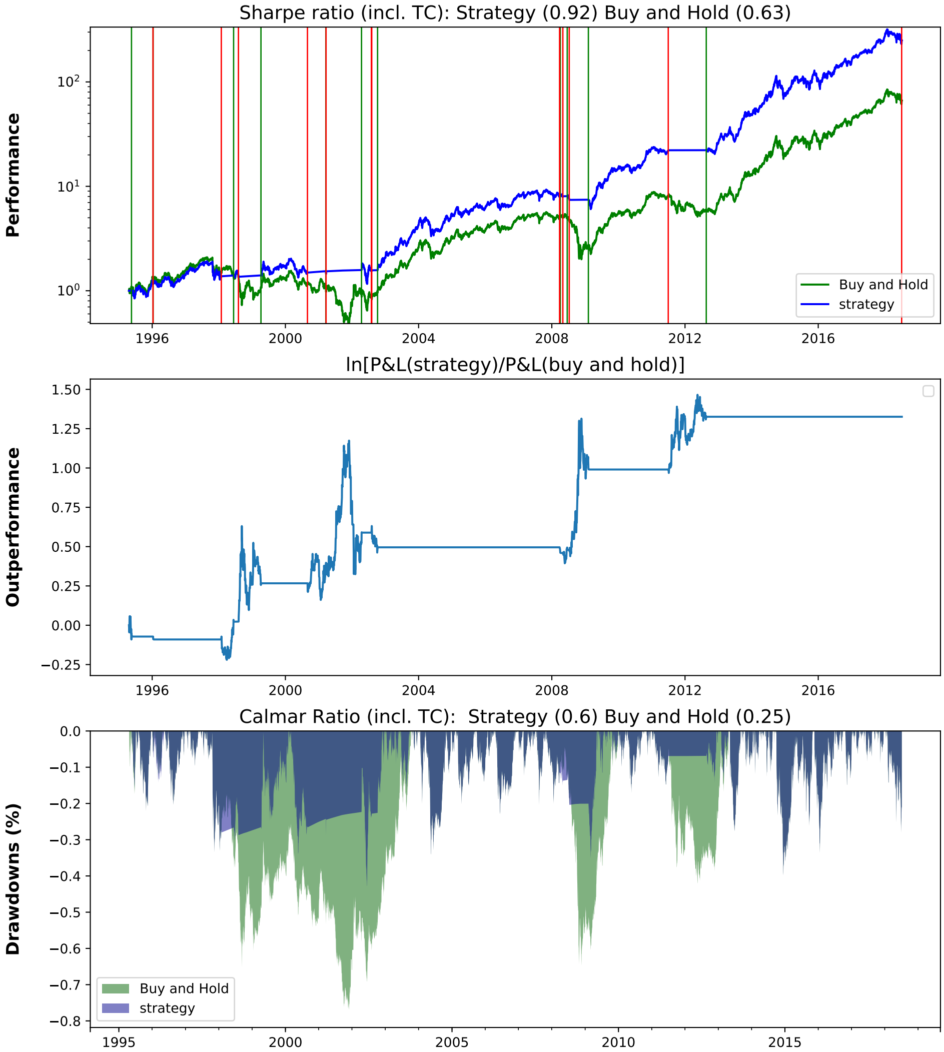

Figure A.2: Performance of the trading strategy for the equity index **ARGENTINA MERVAL** during the time-period *December 1994 - July 2018*. Early Bubble Warning entry threshold $\alpha = 0$.

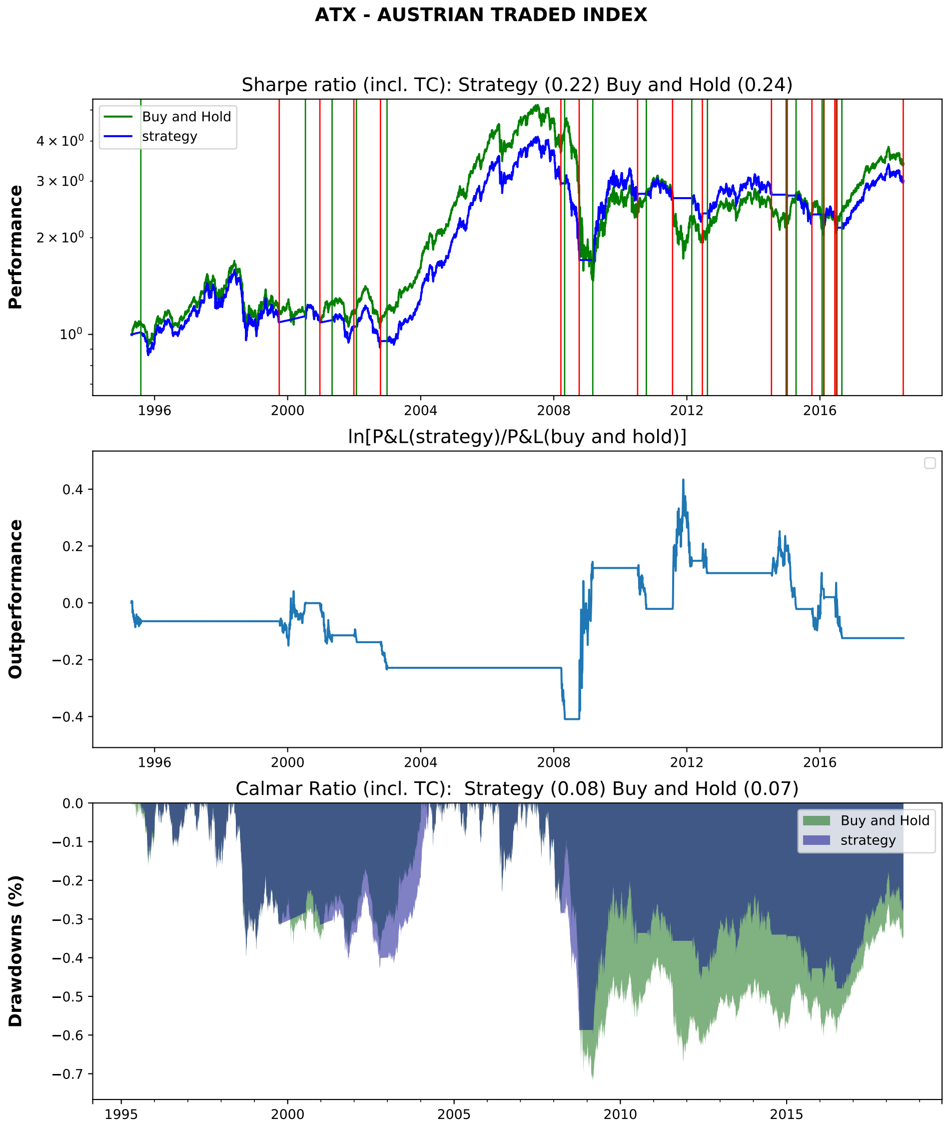

Figure A.3: Performance of the trading strategy for the equity index **ATX** during the time-period *December 1994 - July 2018*. Early Bubble Warning entry threshold $\alpha = -0.01$.

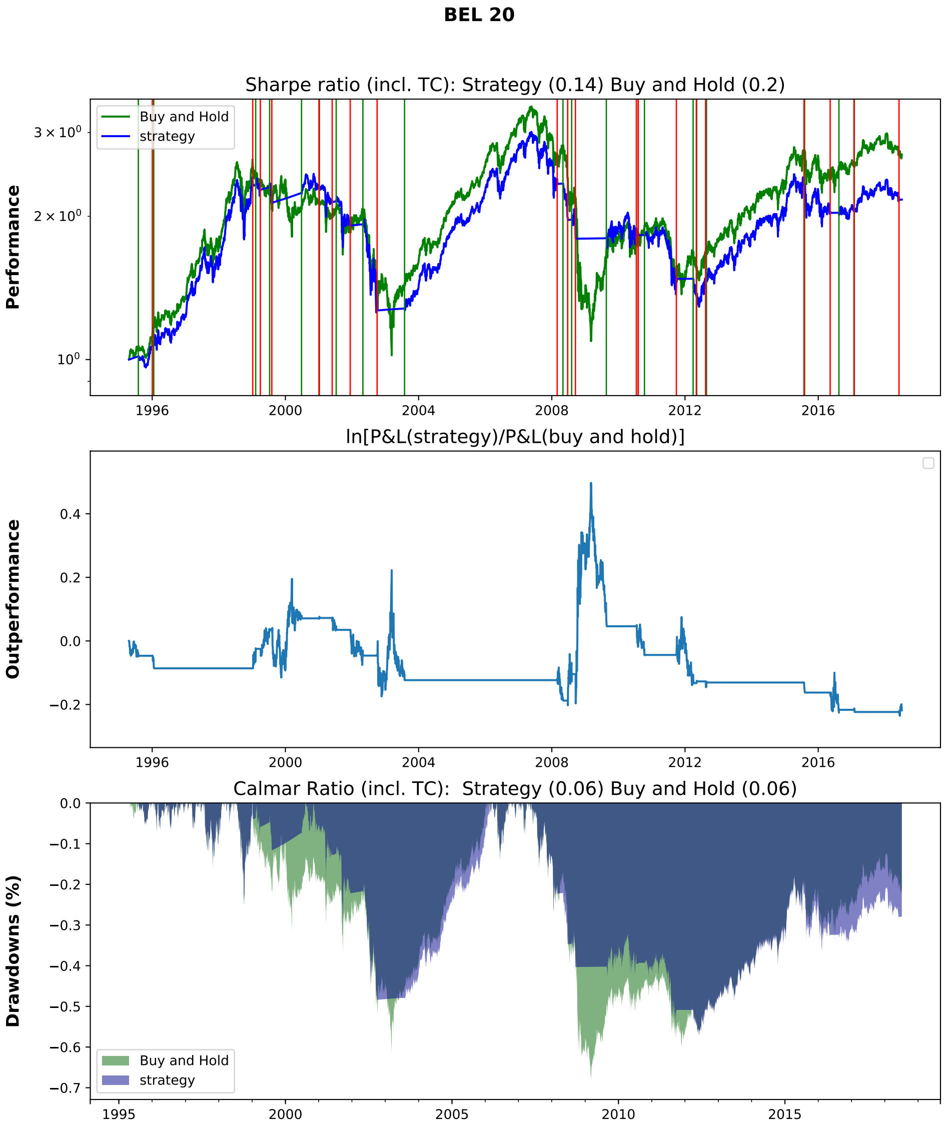

Figure A.4: Performance of the trading strategy for the equity index **BEL 20** during the time-period *December 1994 - July 2018*. Early Bubble Warning entry threshold $\alpha = 0.01$.

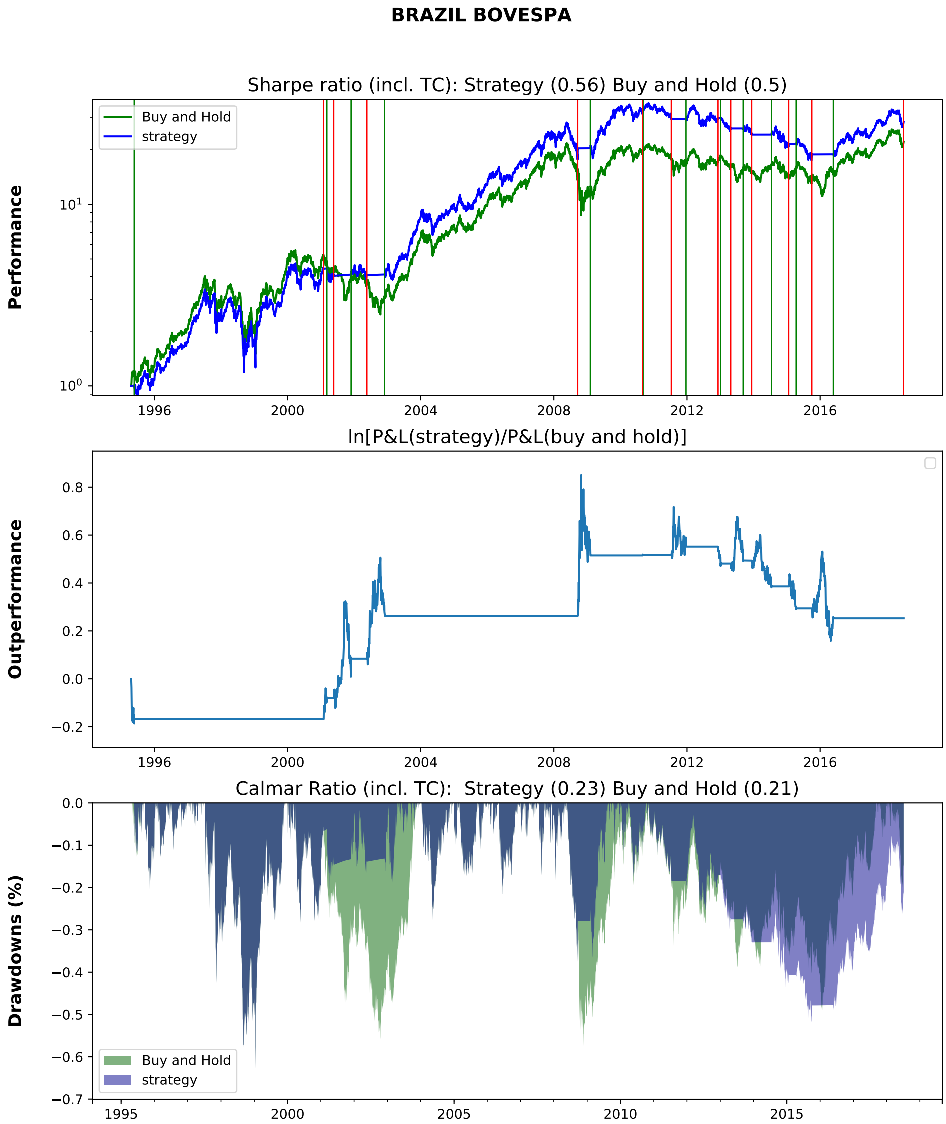

Figure A.5: Performance of the trading strategy for the equity index **BRAZIL BOVESPA** during the time-period *December 1994 - July 2018*. Early Bubble Warning entry threshold $\alpha = -0.01$.

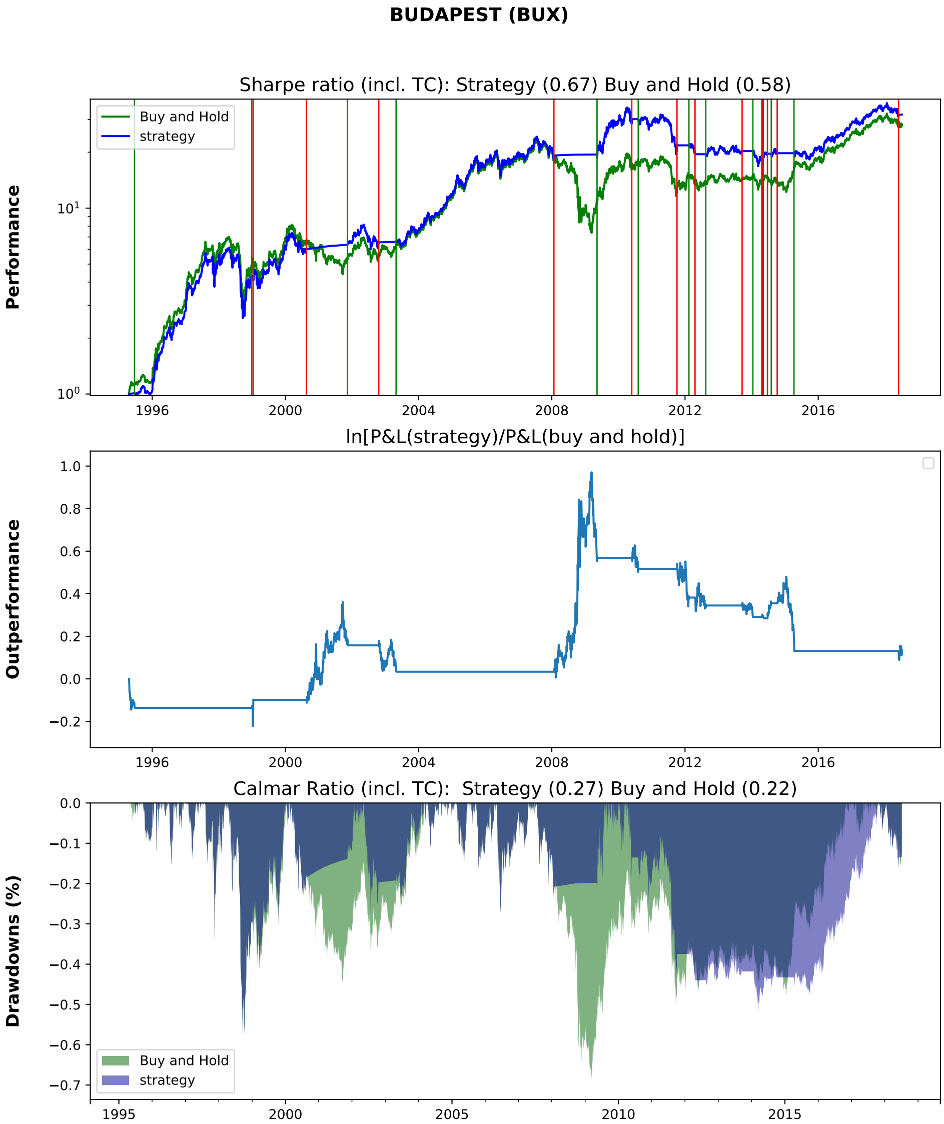

Figure A.6: Performance of the trading strategy for the equity index **BUDAPEST (BUX)** during the time-period *December 1994 - July 2018*. Early Bubble Warning entry threshold $\alpha = 0$.

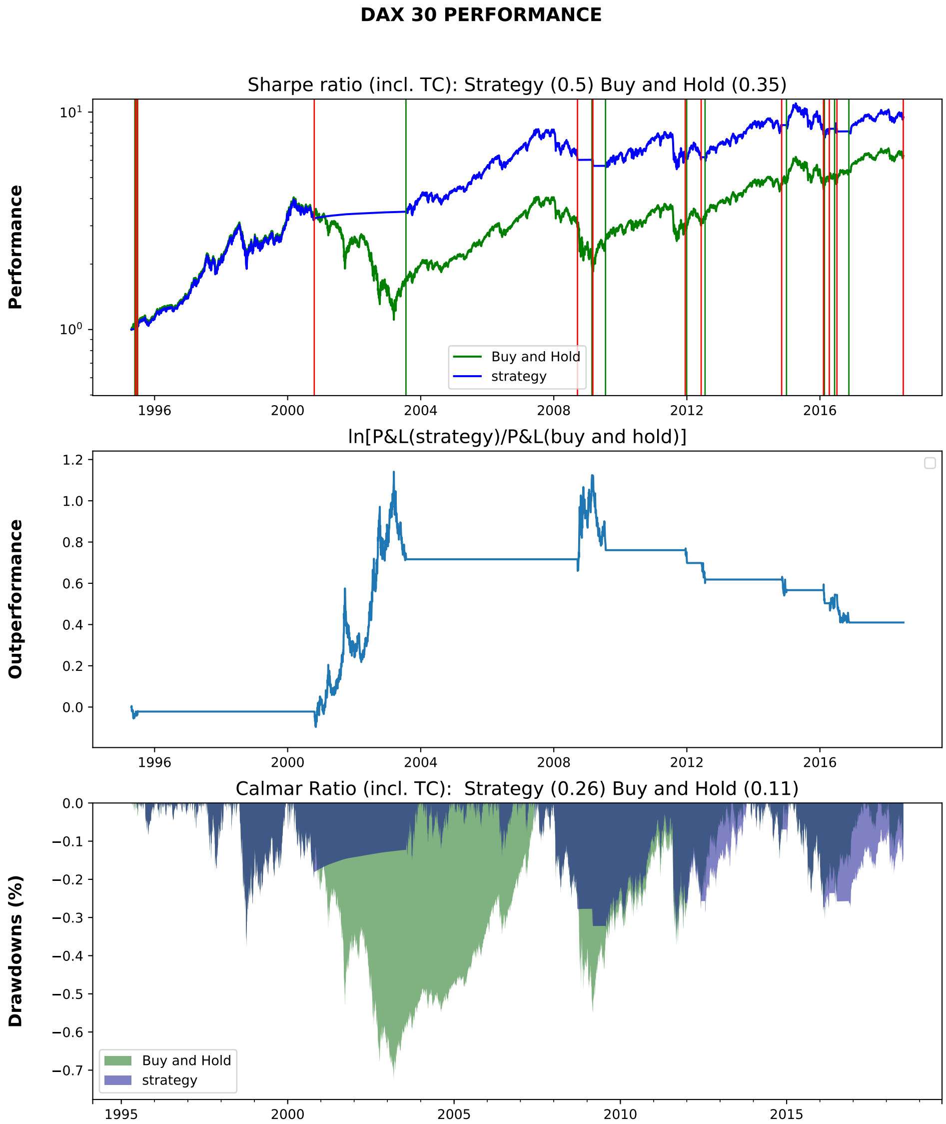

Figure A.7: Performance of the trading strategy for the equity index **DAX** during the time-period *December 1994 - July 2018*. Early Bubble Warning entry threshold $\alpha = 0$.

DOW JONES INDUSTRIALS

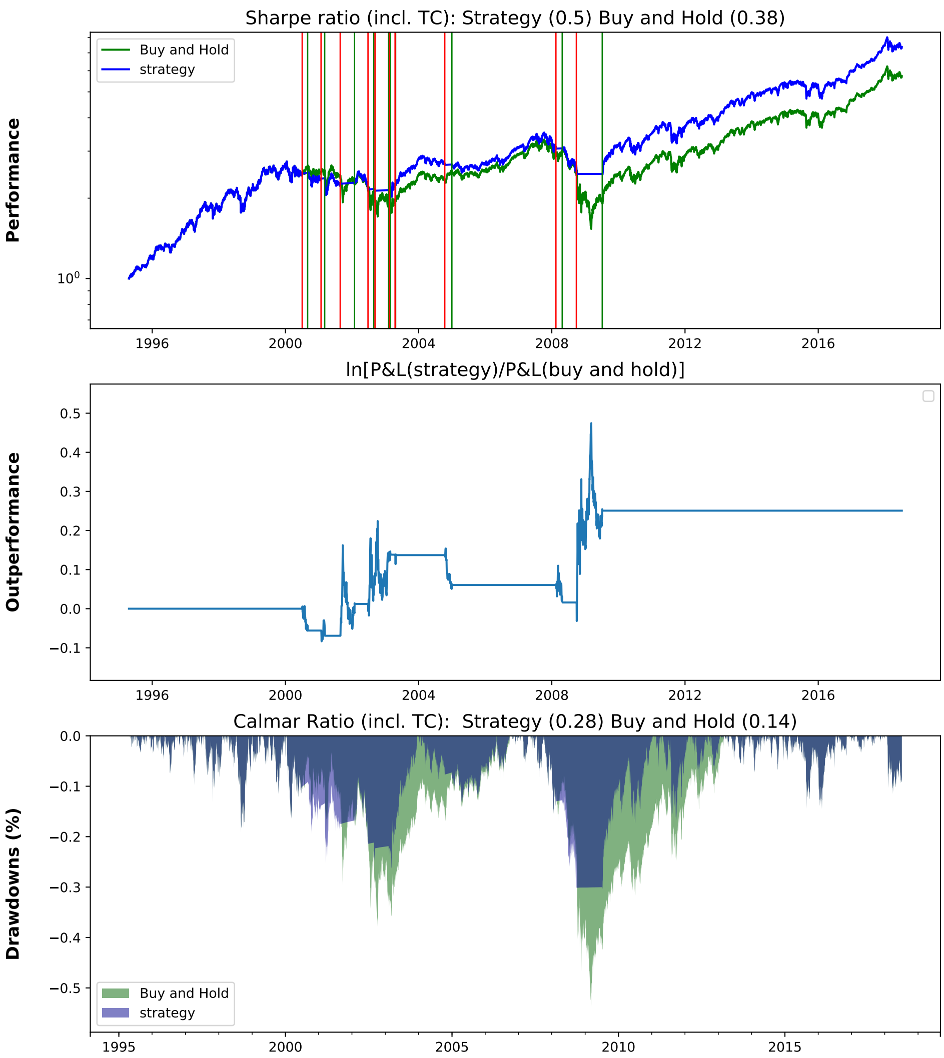

Figure A.8: Performance of the trading strategy for the equity index **DOW JONES INDUSTRIALS** during the time-period *December 1994 - July 2018*.Early Bubble Warning entry threshold $\alpha = -0.01$.

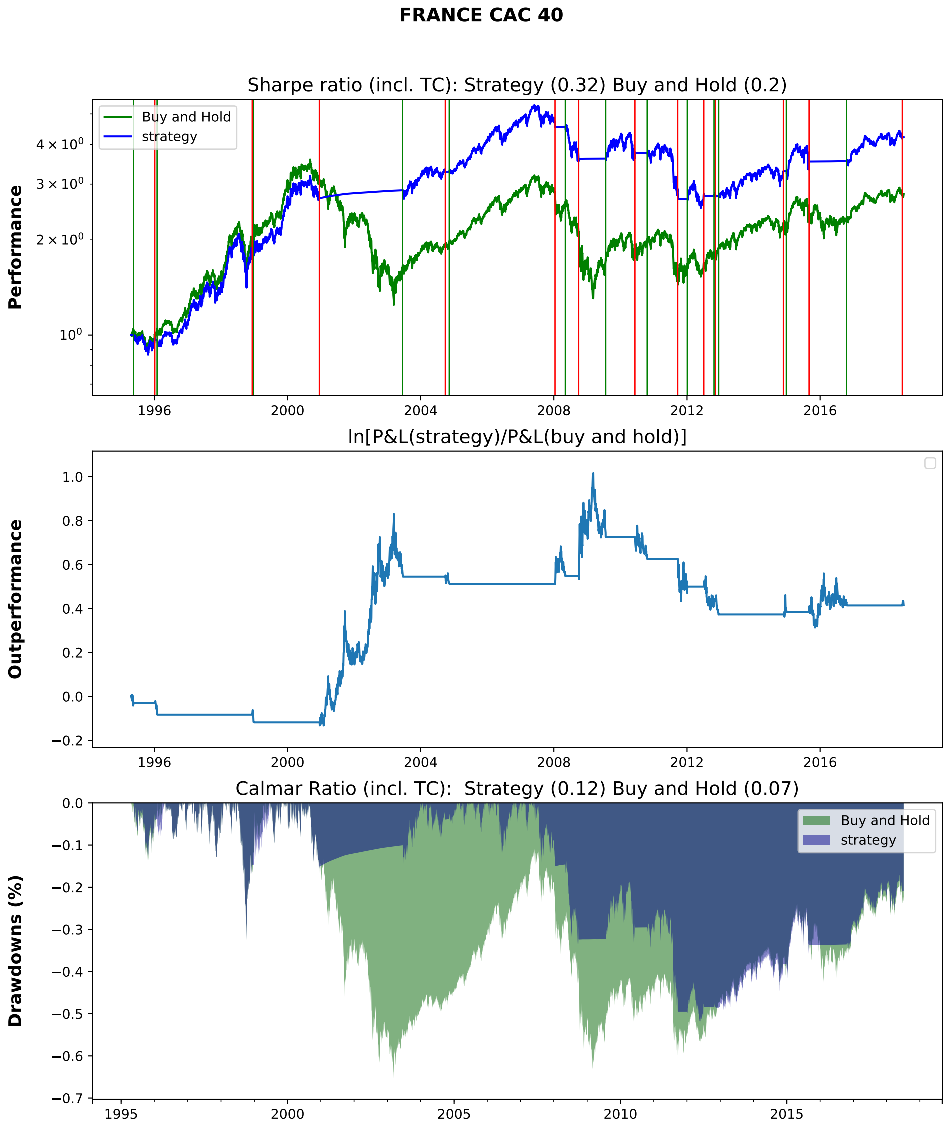

Figure A.9: Performance of the trading strategy for the equity index **FRANCE CAC 40** during the time-period *December 1994 - July 2018*. Early Bubble Warning entry threshold $\alpha = 0.01$.

HANG SENG

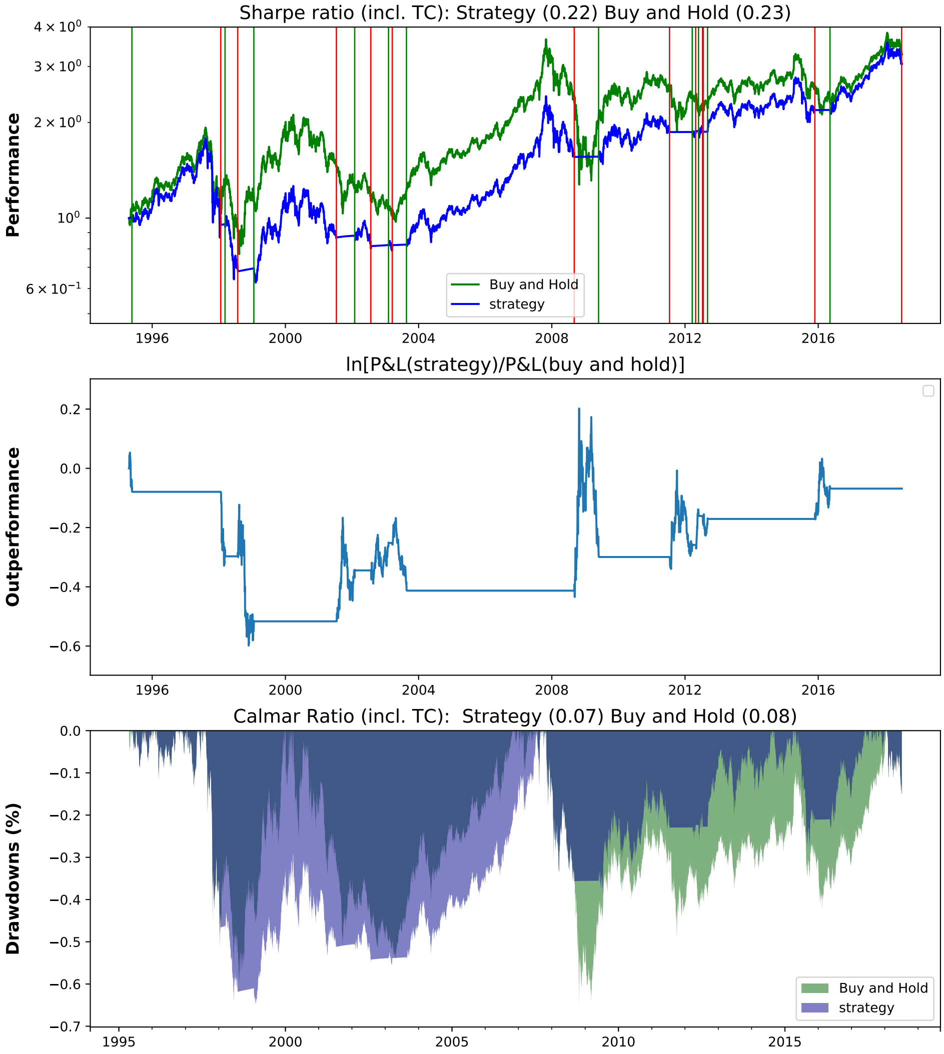

Figure A.10: Performance of the trading strategy for the equity index **HANG SENG** during the time-period *December 1994 - July 2018*. Early Bubble Warning entry threshold $\alpha = -0.01$.

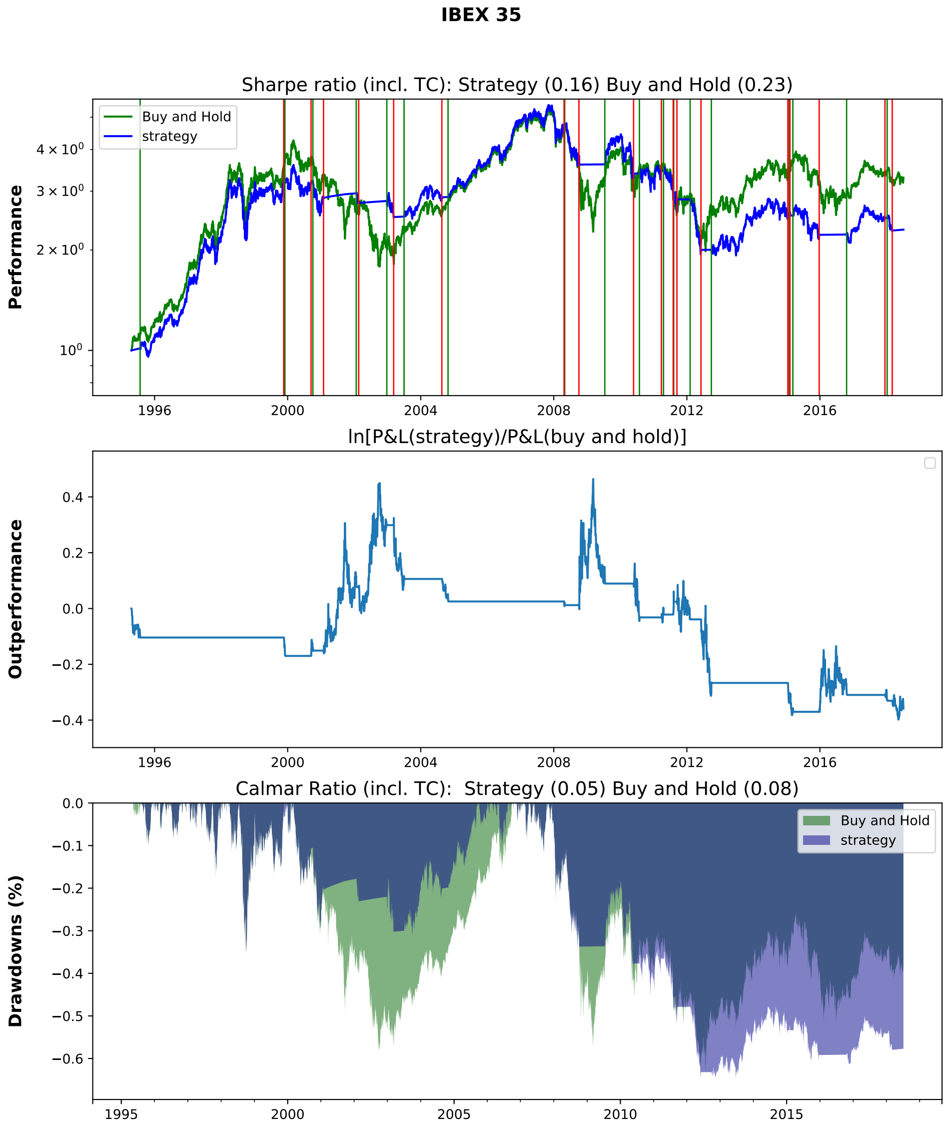

Figure A.11: Performance of the trading strategy for the equity index **IBEX 35** during the time-period *December 1994 - July 2018*. Early Bubble Warning entry threshold $\alpha = 0$ was used.

KOREA SE COMPOSITE (KOSPI)

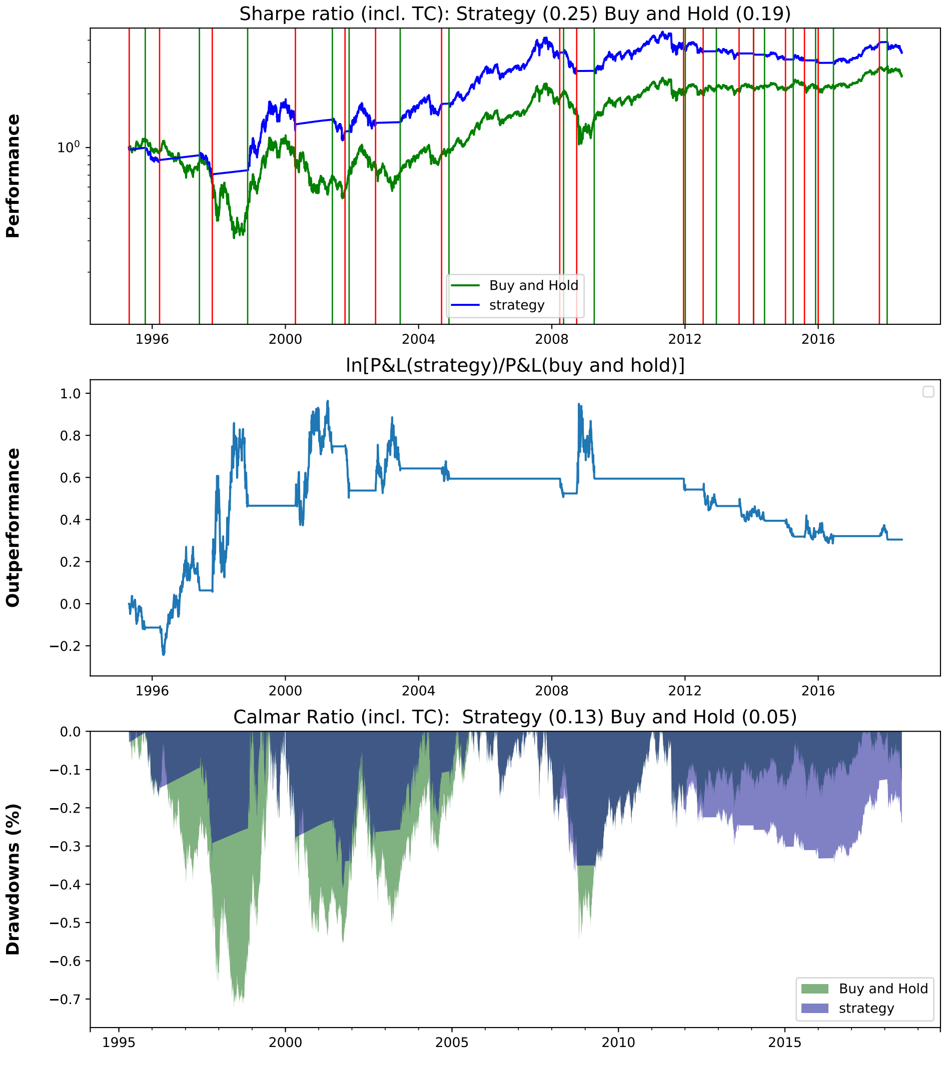

Figure A.12: Performance of the trading strategy for the equity index **KOREA SE COMPOSITE (KOSPI)** during the time-period *December 1994 - July 2018*. Early Bubble Warning entry threshold $\alpha = 0.01$.

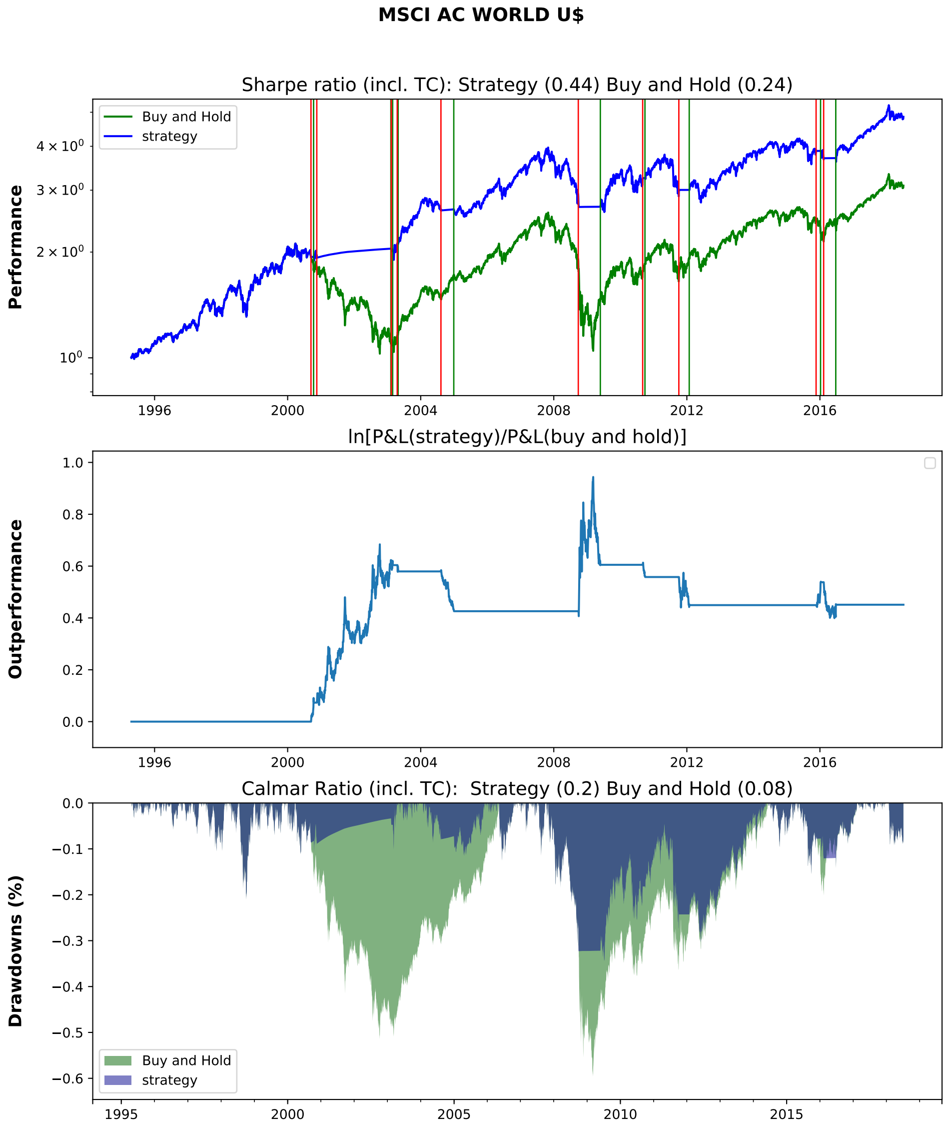

Figure A.13: Performance of the trading strategy for the equity index **MSCI AC WORLD** during the time-period *December 1994 - July 2018*. Early Bubble Warning entry threshold $\alpha = 0.01$.

MSCI WORLD U$

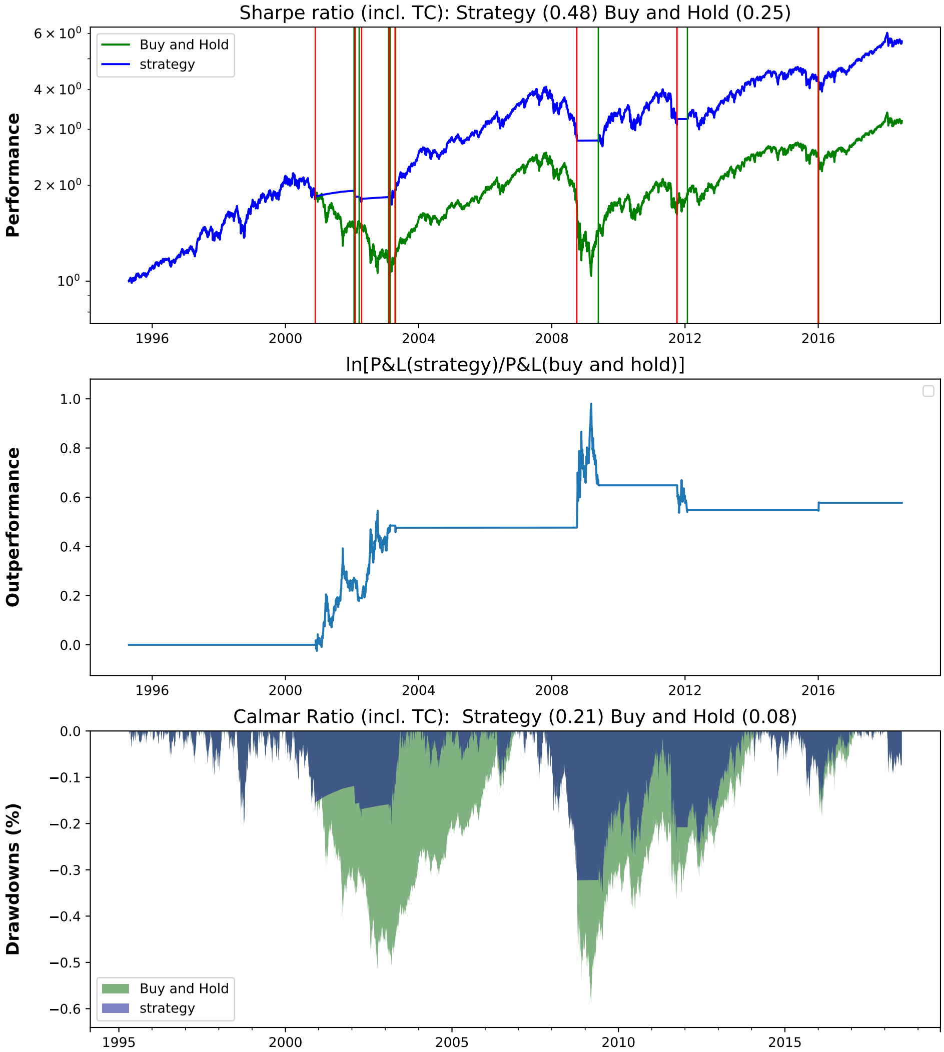

Figure A.14: Performance of the trading strategy for the equity index **MSCI WORLD** during the time-period *December 1994 - July 2018*. Early Bubble Warning entry threshold $\alpha = -0.01$.

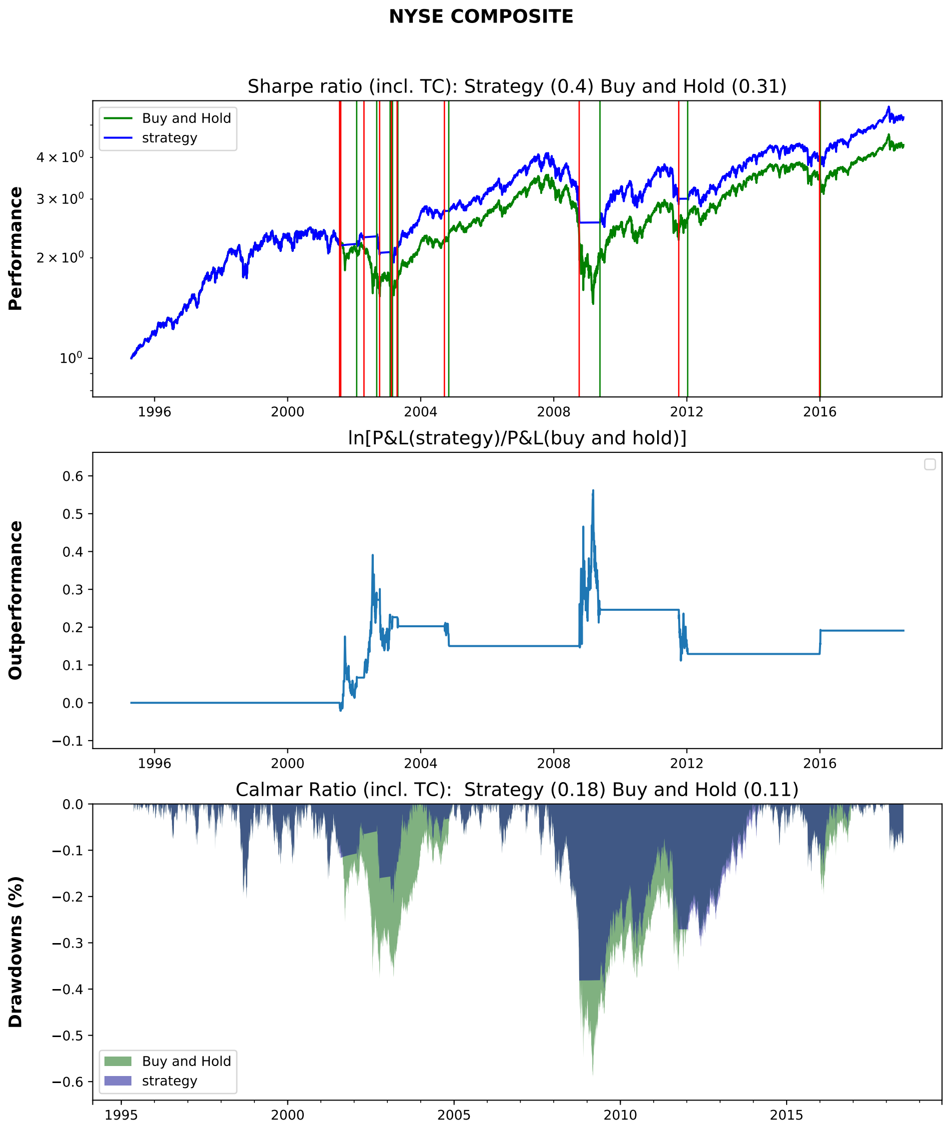

Figure A.15: Performance of the trading strategy for the equity index **NYSE COMPOSITE** during the time-period *December 1994 - July 2018*. Early Bubble Warning entry threshold $\alpha = -0.01$ was used.

OMX STOCKHOLM 30 (OMXS30)

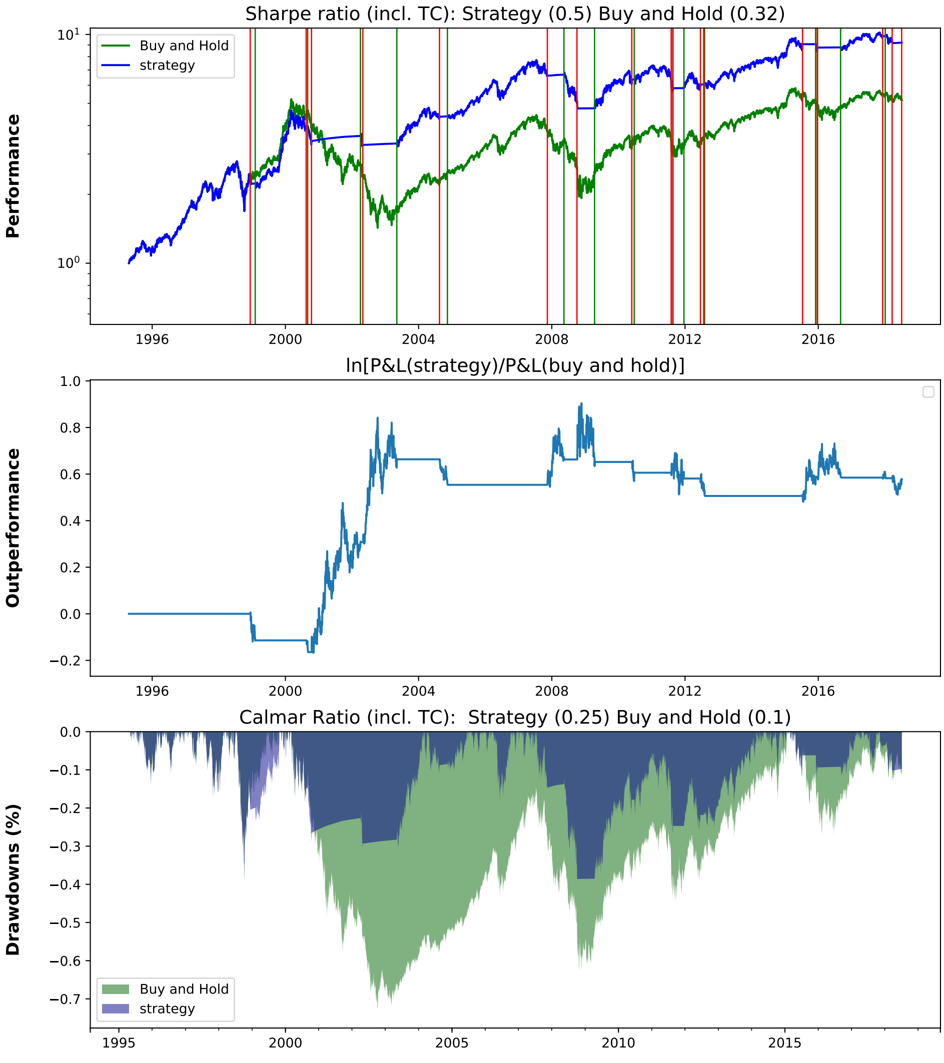

Figure A.16: Performance of the trading strategy for the equity index **OMX STOCKHOLM 30** during the time-period *December 1994 - July 2018*. Early Bubble Warning entry threshold $\alpha = 0.01$ was used.

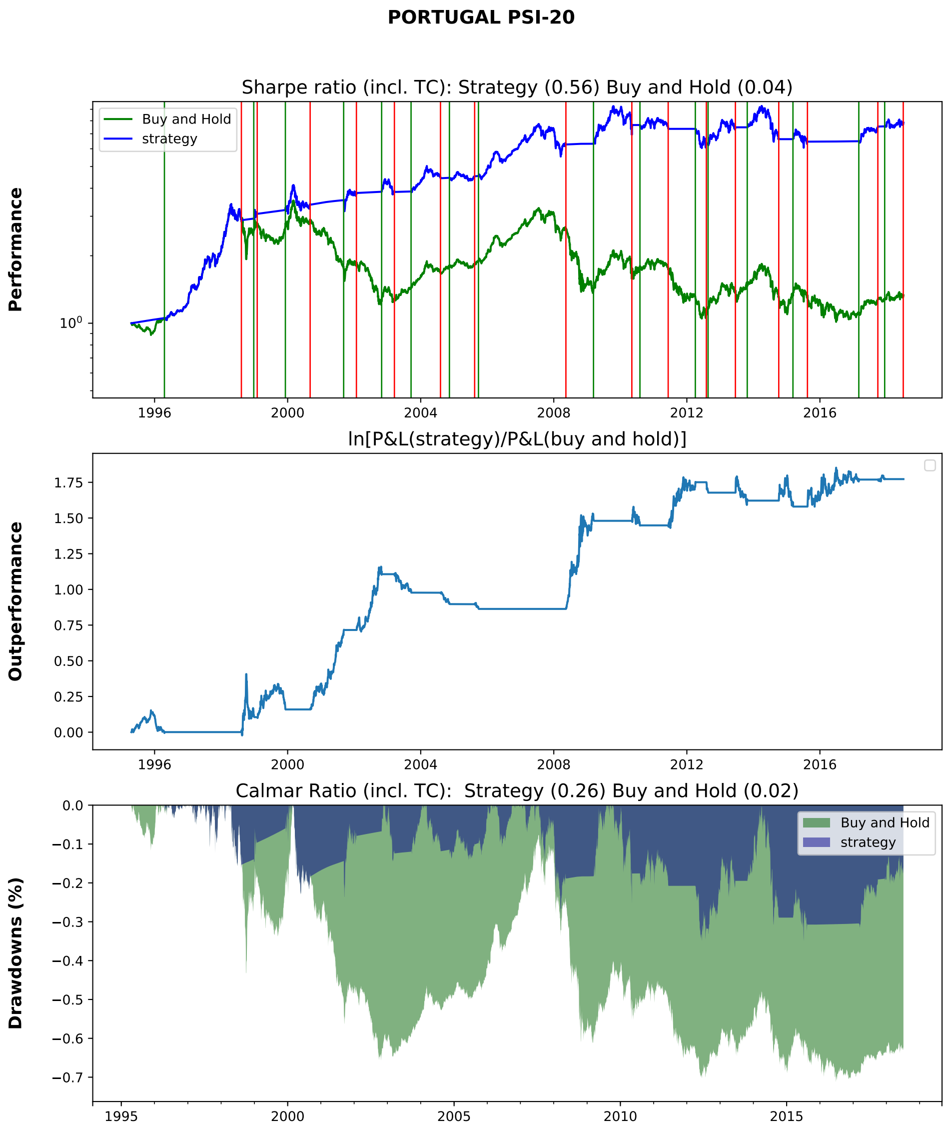

Figure A.17: Performance of the trading strategy for the equity index **PORTUGAL PSI 20** during the time-period *December 1994 - July 2018*. Early Bubble Warning entry threshold $\alpha = 0.01$ was used.

RUSSELL 2000

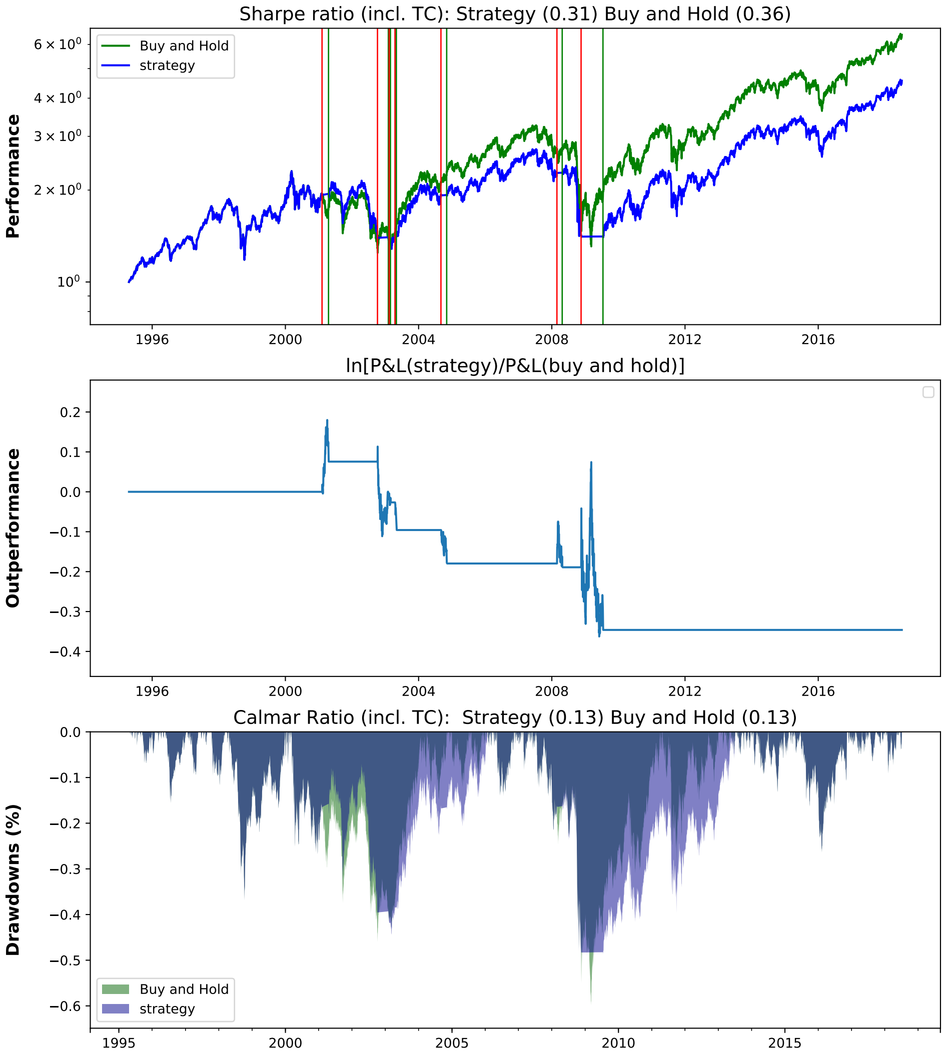

Figure A.18: Performance of the trading strategy for the equity index **RUSSELL 2000** during the time-period *December 1994 - July 2018*. Early Bubble Warning entry threshold $\alpha = -0.01$ was used.

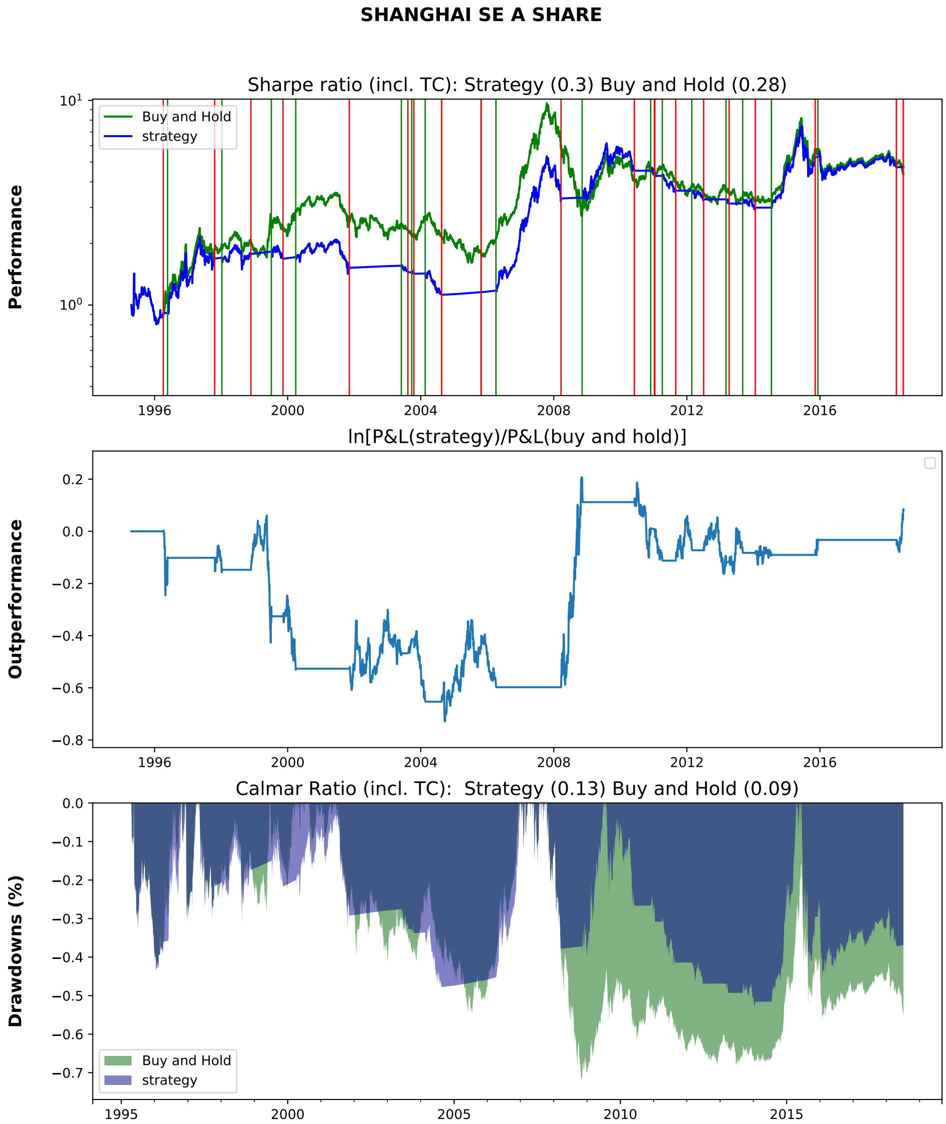

Figure A.19: Performance of the trading strategy for the equity index **SHANGHAI** during the time-period *December 1994 - July 2018*. Early Bubble Warning entry threshold $\alpha = 0.01$.

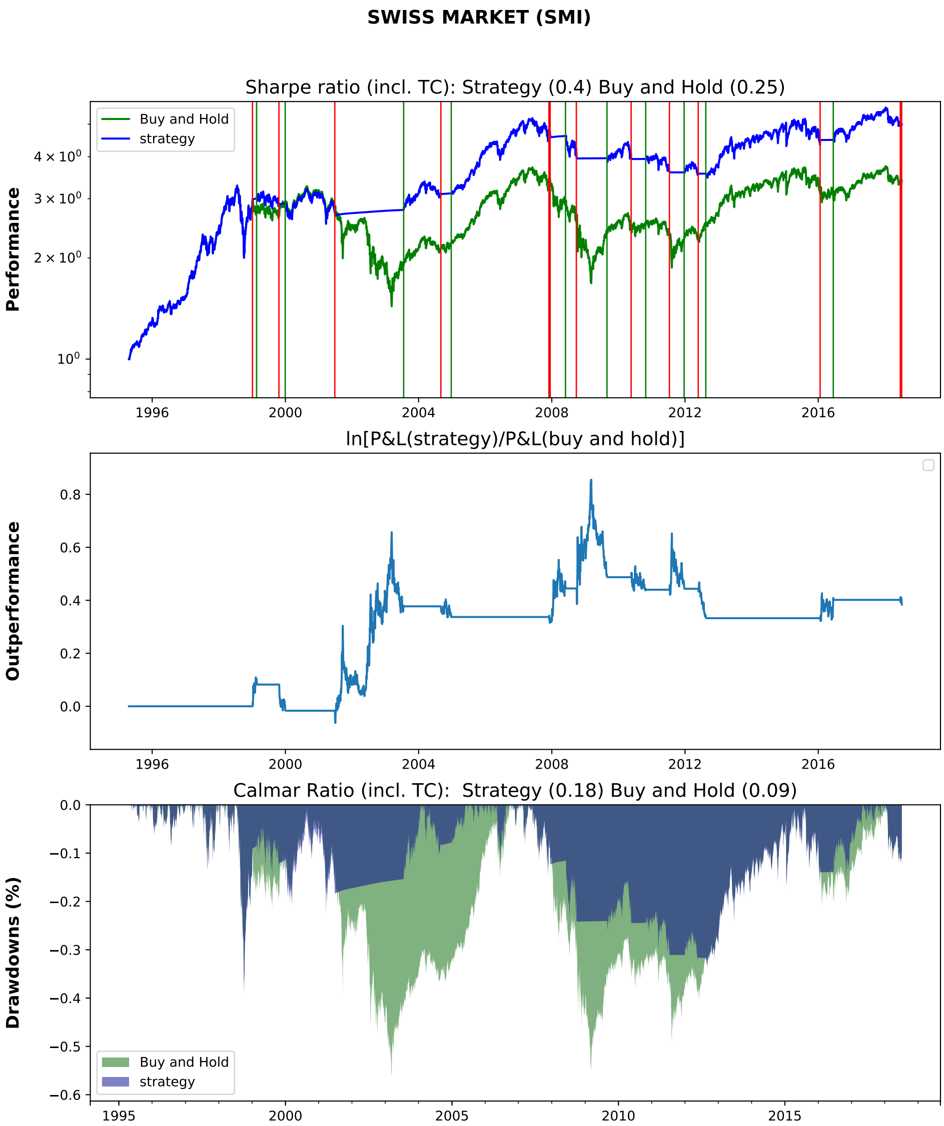

Figure A.20: Performance of the trading strategy for the equity index **SWISS MARKET SMI** during the time-period *December 1994 - July 2018*. Early Bubble Warning entry threshold $\alpha = 0.01$ was used.

Bibliography

[1] G. Demos and D. Sornette. Lagrange regularization approach to compare nested data sets and determine objectively financial bubbles' inceptions. *Swiss Finance Institute Research Paper Series No 18–20*, 2018.

[2] E. Fama. Efficient markets: a review of theory and empirical work. *Journal of Finance*, 25:383–417, 1970.

[3] E. Fama. Efficient capital markets. *Journal of Finance*, 46:1575–1618, 1991.

[4] V. Filimonov and D. Sornette. A stable and robust calibration scheme of the log-periodic power law model. *Physica A: Statistical Mechanics and its Applications*, 392(17):3698–3707, 2013.

[5] Z. Forró, R. Woodard, and D. Sornette. Using trading strategies to detect phase transitions in financial markets. *Physical Review E*, 91(4):042803, 2015.

[6] Z.Q. Jiang, W.X. Zou, D. Sornette, R. Woodard, K. Bastiaensen, and P. Cauwels. Bubble diagnosis and prediction of the 2005-2007 and 2008-2009 chinese stock market bubbles. *Journal of Economic Behavior & Organization*, 74(3):149–162, 2010.

[7] A. Johansen, O. Ledoit, and D. Sornette. Crashes as critical points. *International Journal of Theoretical and Applied Finance*, 3:219–255, 2000.

[8] A. Johansen and D. Sornette. Shocks, crashes and bubbles in financial markets. *Brussels Economic Review*, 53(2):201–253, 2010.

[9] J. M. Keynes. *The General Theory of Employment, Interest and Money*. Palgrave Macmillan, 1936.

[10] N.-P. Pham Huu. Back-testing of trading strategies based on financial crisis observatory output. Master's thesis, ETH Zurich, 2018.

[11] D. Sornette. Dragon-kings, black swans and the prediction of crises. *International Journal of Terraspace Science and Engineering*, 2(1):1–18, 2009.

[12] D. Sornette and P. Cauwels. The illusion of the perpetual money machine. *Swiss Finance Institute Research Paper No. 12-40*, 2012.

[13] D. Sornette and P. Cauwels. Financial bubbles: mechanisms and diagnostics. *Review of Behavioral Economics*, 2(3):279–305, 2015.

[14] D. Sornette, G. Demos, Q. Zhang, P. Cauwels, V. Filimonov, and Q. Zhang. Real-time prediction and post-mortem analysis of the shanghai 2015 stock market bubble and crash. *Journal of Investment Strategies*, 4(4):77–95, 2015.

[15] D. Sornette and V. Filimonov. Power law scaling and "dragon-kings" in distributions of intraday financial drawdowns. *Chaos, Solitons & Fractals*, 74:27–45, 2015.

[16] D. Sornette and A. Johansen. Significance of log-periodic precursors to financial crashes. *Quantitative Finance*, 1(4):452–471, 2001.

[17] D. Sornette and W.X. Zhou. Predictability of large future changes in major financial indices. *International Journal of Forecasting*, 22:153–168, 2006.

[18] N.-N. Taleb. *The Black Swan: the impact of the highly improbable*. London: Penguin, 2012.

[19] W. Yan, R. Rebib, R. Woodard, and D. Sornette. Detection of crashes and rebounds in major equity markets. *International Journal of Portfolio Analysis and Management*, 1(1):59–79, 2012.